

ADA030924



UCLA-ENG-7672
JULY 1976

**WAVES AND INSTABILITIES IN STEADY-STATE
HIGH-BETA PLASMAS**

Principal Investigator: N.C. LUHMANN, JR.
Assistant Professor

Co-Principal Investigator: F.F. CHEN
Professor

AIR FORCE OFFICE OF SCIENTIFIC RESEARCH (AFSC)

NOTICE OF TRANSMITTAL TO DDC

This technical report has been reviewed and is approved for public release IAW AFR 190-12 (7b). Distribution is unlimited.

A. D. BLOSE

Technical Information Officer

Unclassified

SECURITY CLASSIFICATION OF THIS PAGE (When Data Entered)

REPORT DOCUMENTATION PAGE		READ INSTRUCTIONS BEFORE COMPLETING FORM	
1. REPORT NUMBER AFOSR-TR-76-110 I	2. GOVT ACCESSION NO.	3. RECIPIENT'S CATALOG NUMBER 9	
4. TITLE (and Subtitle) WAVES AND INSTABILITIES IN STEADY-STATE HIGH-BETA PLASMAS,		5. TYPE OF REPORT & PERIOD COVERED Final Report, 15 May 72 - May 15, 1972/30 June 1976	
7. AUTHOR(s) N. C. Luhmann, Jr.		6. PERFORMING ORG. REPORT NUMBER 7672	
8. AUTHOR(s) (continued) N. C. /Luhmann, Jr. Francis F./Chen		8. CONTRACT OR GRANT NUMBER(s) US AFOSR Grant 72-2339	
9. PERFORMING ORGANIZATION NAME AND ADDRESS Department of Electrical Sciences 7731 Boelter Hall, University of California Los Angeles, California 90024		10. PROGRAM ELEMENT, PROJECT, TASK AREA & WORK UNIT NUMBERS 9751-03 6462 F	
11. CONTROLLING OFFICE NAME AND ADDRESS Department of the Air Force Air Force Office of Scientific Research (NP) Bolling Air Force Base, DC 20332		12. REPORT DATE July 1976	
14. MONITORING AGENCY NAME & ADDRESS (if different from Controlling Office) 12 61 p.		13. NUMBER OF PAGES 60	
		15. SECURITY CLASS. (of this report) Unclassified	
		15a. DECLASSIFICATION/DOWNGRADING SCHEDULE	
16. DISTRIBUTION STATEMENT (of this Report) Approved for public release; distribution unlimited			
14 UCLA-ENG-7672 15 VAF-AFOSR-2339-72			
17. DISTRIBUTION STATEMENT (of the abstract entered in Block 20, if different from Report) 16 AF-9751 17 975103			
18. SUPPLEMENTARY NOTES TECH, OTHER			
19. KEY WORDS (Continue on reverse side if necessary and identify by block number) Finite Beta Waves and Instabilities Steady-State, High-Density, Fully-Ionized Plasma Sources Finite-Bandwidth Pump Control of Parametric Instabilities Drift-Alfvén Instability Electromagnetic Ion Cyclotron Instability			
ABSTRACT (Continue on reverse side if necessary and identify by block number) The generation of steady-state, high-density, fully-ionized plasmas in magnetically confined arcs and arc jets has been studied. Finite-beta waves and instabilities appropriate to the ionospheric and magnetospheric plasmas have been investigated. Anomalous resistivity due to instability produced turbulent fluctuations has been studied. Experimental simulations of laser-plasma interactions have been performed in the microwave region.			

DD FORM 1 JAN 73 1473

EDITION OF 1 NOV 65 IS OBSOLETE
S/N 0102-LF-014-0001

SECURITY CLASSIFICATION OF THIS PAGE (When Data Entered)

409432 6B

TABLE OF CONTENTS

	<u>PAGE</u>
I. INTRODUCTION AND PURPOSE OF RESEARCH PROGRAM	1
II. ACHIEVEMENTS OF UCLA PLASMA ENGINEERING LABORATORY UNDER US AFOSR FUNDING	4
III. PROGRESS: JULY 1, 1975 TO JUNE 30, 1976	9
A. Drift-Alfvén Instability	9
B. Laser-Plasma Interaction Studies	11
1. Finite Bandwidth Pump Production	14
2. Effect of Finite Pump Bandwidth on the Parametric Decay Instabilities	17
3. 10 cm Finite Bandwidth Heating Experiment	32
C. Current - Driven Electromagnetic Ion Cyclotron Instability . . .	39
1. Theory	39
2. Experiment	42
D. Nonlinear Evolution and "Anomalous" Resistivity	44
E. Plasma Source Development	44
1. Arcjet Plasma	44
2. Electrostatically Confined, Unmagnetized Plasma	45
3. Differentially Pumped, Large Diameter, Finite-Beta Magnetized Plasma	46
IV. PUBLICATIONS AND PRESENTATIONS: JULY 1, 1975 TO JUNE 30, 1976 . . .	47
V. RESEARCH PERSONNEL	49
VI. REFERENCES	49

I. Introduction and Purpose of Research Program

Our program has branched out from a study of finite-beta waves and instabilities, but continues to have as its purpose the basic study of plasma waves and instabilities appropriate to Air Force problems. The present areas under investigation in this laboratory under this grant include the following:

A. The generation of steady-state, high-density, fully-ionized plasmas in magnetically confined arcs and arc jets. These have been of great use in our study of finite-beta waves and instabilities and may also be of use as target plasmas for use in laser plasma heating.

B. The study of finite beta waves and instabilities appropriate to the ionospheric and magnetospheric plasmas where satellite observations indicate that the β ranges from $\sim 10\%$ to a value in excess of unity. A knowledge of the magnetospheric plasma, in particular the waves and instabilities it may support, is necessary for many diverse reasons. Details concerning the mechanisms for equatorial spread F require further elucidation. Communications, weather and other satellites operate in the magnetospheric plasma environment at the geosynchronous orbit (~ 6.6 earth radii). Arc-related deterioration of the spacecraft surfaces, systems failures and telemetry anomalies have been attributed to kilovolt electrons associated with the "substorm" phenomenon. Substorms are thought to be caused by instabilities in the geomagnetic tail.¹ Waves and instabilities in the magnetosphere also affect the ionosphere indirectly by producing energetic particle precipitation. Hence VLF and radio transmissions in the earth-ionosphere waveguide can be perturbed by instabilities at high altitudes.² Our investigations of both the drift-Alfvén and current-driven electromagnetic ion cyclotron instability are examples of work in this area.

C. The presence of instability produced turbulent fluctuations can greatly enhance the resistivity of a plasma beyond the Spitzer-Härm value. As mentioned in Section IIIC, this "anomalous" resistivity can result in the presence of magnetic field aligned electric fields which are of great importance in the production of auroral arcs. In addition, the enhanced resistivity can greatly increase the absorption and heating in laser-plasma interactions. We have therefore decided to devote some of our energies to this important area.

D. The use of high power lasers to heat critical density plasmas and solenoidally confined underdense plasmas is presently being investigated as a possible source of soft x-rays. We are investigating questions pertaining to this scheme both with our own high power CO₂ laser chain (ERDA) and by simulation of the interaction in the microwave region (AFOSR) where well-diagnosed plasmas and high power sources are easily obtainable. In particular, our work on the effects of a finite-bandwidth pump field on the parametric instability is described in Section IIB. We have investigated both the effects of such a pump on the instability threshold, but also on the production of hot electron tails.

Our approach to the above-mentioned problems has been to design easily interpretable laboratory wave experiments which would elucidate the key features of the phenomena under investigation. Of primary importance in this work has been the existence of well-diagnosed, reasonably quiescent plasma sources. This was particularly important in the drift-Alfven study and our present arcjet device is perhaps the finest steady-state high-beta plasma source in the world. This unique facility has achieved an international reputation and for the second year we have had a foreign scientist spend the summer collaborating on our AFOSR work at no cost to the grant. During the summer of 1975, the position was occupied by Prof. K.F. Lee of the

Chinese University of Hong Kong who shared in our theoretical work on the electromagnetic ion cyclotron instability. Presently, Professor R. Armstrong of Tromsø University (Norway) is working with us on our experimental program.

Our progress over the entire grant period is summarized in Section II. Our progress over the past year is discussed in Section III. The identification and properties of the drift-Alfvén instability are covered in Section IIIA. A detailed paper concerning the theoretical dispersion and experimental verification has been accepted for publication in Physics of Fluids. Temperature fluctuations and wave-induced losses associated with this instability have been measured and are the subject of a paper to be published in the Journal of Applied Physics. Our work on the effects of a finite bandwidth driver pump on the threshold, growth rate, saturation level and heating of the parametric decay instability is reviewed in Section IIIB. This has important implication for proposed schemes for laser heating of plasmas. Finally, our investigations concerning the electromagnetic ion cyclotron (EMIC) instability are described in Section IIIC. Our brief study of anomalous resistance is discussed in Section IIID. Finally, the plasma source development conducted in support of the various projects is summarized in Section IIIE.

SECTION II

ACHIEVEMENTS OF UCLA PLASMA ENGINEERING LABORATORY UNDER US AFOSR FUNDING

The following list constitutes the major achievements and milestones that have occurred under our US AFOSR sponsored research during the period of May 15, 1971 to the present (Grants #71-2080 and 72-2339). Only the basic published references are given except in the case of our current work where APS Bulletin references are also indicated. We have lumped papers into general topic headings so that, for example, four separate investigations are listed under (5). In addition to the work listed herein, which is directly attributable to US AFOSR funding, many studies which impact on areas of Air Force interest have also been conducted under the auspices of other agencies. A good example of this is our ERDA supported study of Brillouin backscattering (J. J. Turechek and F. F. Chen, Phys. Rev. Lett., 36,720 (1976) which is of great importance to proposed soft x-ray sources using CO₂ laser-heated plasmas. Air Force funds have therefore in a real sense been effectively increased by the presence of funding from other agencies.

(1) Development of a Dense, Fully-Ionized, Current-Free, Steady-State, Quiescent Finite-Beta Plasma Source

From the outset of this grant, one of the primary aims was the development of a plasma source which would permit the same careful study of finite-beta waves and instabilities as the Q-machine allowed for the low- β case. This effort was quite successful and resulted in the UCLA arcjet device (J. T. Tang et al., J. Appl. Phys. 46, 3376, (1975)). This is perhaps the finest such facility in the world and is beginning to attract international interest. We have had foreign visitors working on this device the past two summers (at no cost to AFOSR) and beginning

January, 1976 Dr. Armstrong of Tromso, Norway will be spending a year with us working on magnetospheric related problems. Several groups are now constructing identical devices including Y. Nishida of Utsunomiya University, Japan and M. Yamada of Princeton University. In addition, R. P. H. Chang of Bell Laboratories is constructing a similar device. This is an extremely reliable device permitting us to concentrate on the study of waves and instabilities which pertain to the magnetospheric plasma.

(2) Development of a Fully-Ionized, Steady-State, High-Density Magnetized Arc Column for Laser-Plasma Interaction Studies

To permit the careful investigation of high power CO₂ laser interactions with plasmas, a steady-state high density arc column was developed (D. T. Jassby, J. Appl. Phys. 43, 4542 (1972)). This carefully diagnosed device produces a plasma of density $n_e \approx 3 \times 10^{16} \text{ cm}^{-3}$ and temperature $T_e \approx T_i = 1.6\text{eV}$.

(3) Heat Flow Measurements in a Laser-Heated Magnetically Confined Plasma

Of great importance to proposed CO₂ laser heating of dense plasmas is the mechanism and rapidity of thermal conduction from the region of energy absorption. Measurements of perpendicular and parallel heat conductivity were made using a CO₂ TEA laser to heat the above-mentioned arc column (S. W. Fay and D. L. Jassby, Physics Letters 42A, 261 (1972)).

(4) Infrared-Laser Heating of Dense Arc Plasmas

A theoretical study of the feasibility of the use of a dense steady-state arc column as a target plasma for soft x-ray production was made (D. L. Jassby, Phys. Fluids, 15, 2442 (1972)). It was concluded that such plasmas could be heated to 116 eV temperature using 1 GW 10.6 μm radiation with the maximum temperature limited by the rapid thermal conduction.

(5) Experimental Identification of the Drift-Alfvén Instability

It has been long predicted that when the beta of a plasma exceeds the electron-ion mass ratio drift waves can couple to Alfvén waves of comparable phase velocity resulting in instability. This instability has been invoked to explain hydromagnetic oscillations in the post-midnight regions of the auroral boarding of the magnetosphere in addition to equatorial spread F observations. Using the AFOSR supported arc jet device we made the first conclusive identification of this instability (J. T. Tang et al., Phys. Rev. Lett. 34, 70, (1975)). A detailed paper concerning the properties of this instability has been accepted for publication in Physics of Fluids. We have also just completed a detailed study of the temperature fluctuations and wave-induced losses associated with the instability, and a paper describing this study will be published in the Journal of Applied Physics. A final study of the growth and non-linear saturation of this instability is under way.

(6) Electromagnetic Ion Cyclotron Instability

It has long been recognized that when the axial current flowing along the confining magnetic field in a low- β plasma is increased beyond a threshold value, the electrostatic ion cyclotron instability is excited. Forslund et al. (UCLA Report 12-87, 1971) have shown that even for modest values of β ($\approx 1\%$), an electromagnetic ion cyclotron (EMIC) instability has a lower threshold than either the electrostatic ion cyclotron instability or the ion acoustic instability. Such instabilities are of importance as they may give rise to space-craft charging of satellites located at the geosynchronous orbit. They can also affect VLF and radio transmissions by producing energetic particle precipitation. We have therefore begun a study of EMIC instability in our collisional plasma and papers concerning the linear theory have been

accepted for publication in Plasma Physics and also IEEE Transactions on Plasma Science. An experimental study of a spontaneously occurring EMIC instability in our arc jet device is continuing and an article will be submitted for publication shortly.

(7) Use of Infrared Lasers in Feedback Stabilization

In addition to their use in plasma diagnostics and heating, it is proposed to use powerful infrared lasers in the feedback stabilization of magnetically confined plasmas (F. F. Chen, Comments on Plasma Phys, and Controlled Fusion 1, 81, (1972)). In this "double-resonance" scheme a nonlinear coupling occurs when a laser of frequency corresponding to a high frequency resonance is modulated at a frequency equal to a low frequency resonance.

(8) Investigation of Finite-Bandwidth Driver Pump Effects on Parametric Instabilities

Parametric instabilities of both the absorptive and reflective types may have serious consequences for proposed laser heating of large solenoidally confined plasmas and dense plasma focuses. In particular, the reflective instabilities (stimulated Brillouin and Raman scattering) may scatter the incoming laser radiation with obvious deleterious effects. There has therefore been considerable interest in means to increase the thresholds and reduce the growth rates for these instabilities. A proposed solution is to increase the bandwidth of the pump source so that the effective energy within the instability resonance width is reduced. Although there have been extensive analytical and numerical investigations of this point, there has unfortunately not been any experimental verification. Therefore, as part of our growing effort in microwave simulation of laser-plasma interactions, we have undertaken the experimental investigation

of the effects of a finite bandwidth pump on the threshold, growth rate, and saturation of the parametric decay instability. We presented the first such results at Florida (N. C. Luhmann, Jr. et al, B.A.P.S. 20, 1361 (1975)) and a first article describing this work has been published in Physical Review Letters (PRL 36, 1309 (1976)). It should be noted that this work was completed at essentially no cost to AFOSR beyond the transfer of several pieces of government equipment to our grant. The entire cost of the plasma device used in these studies was borne by the University. More recently, we have investigated the effects of finite bandwidth on tail production as discussed in Section III. This work was presented at the Anomalous Absorption Conference at Vancouver and is presently being prepared as a paper to be submitted to Applied Physics Letters. In addition to this work, we are now beginning a complete microwave investigation of the reflective instabilities, which will include threshold, growth rates, nonlinear saturation and methods of control including use of a finite bandwidth driver.

SECTION III

PROGRESS: JULY 1, 1975 TO JUNE 30, 1976

This has been an extremely productive year. In addition to successful investigation of the topics mentioned in our research proposal, we have been able to complete several other tasks.

A. Drift-Alfvén Instability

The identification and study of this instability produced by a coupling of drift and Alfvén waves in our finite β plasma was completed during this grant period. The results were first published in abbreviated form in Physical Review Letters. The complete work constituted the Ph.D. thesis for John Tang and appeared as UCLA Engineering Report No. 7486. A detailed report of our results has been accepted for publication in Physics of Fluids.

We have also completed a study of the temperature fluctuations and wave induced losses associated with this instability. One of the primary features of a drift wave which is used in its identification is the magnitude and phase difference of the density \tilde{n}/n_0 and plasma potential $\tilde{\phi}_p/KT$ fluctuations. Due to the ease with which floating potential ϕ_f measurements are made, it has been common practice to simply compare $\tilde{n} - \tilde{\phi}_f$ fluctuations. However, only in the case of an isothermal plasma without temperature fluctuations is it correct to equate plasma potential $\tilde{\phi}_p$ and floating potential $\tilde{\phi}_f$ fluctuations. Surprisingly, with the exception of some preliminary measurements reported by Müller, et al.³ in a collisional plasma and by N. Abdel Shahid et al.⁴ in a collisionless plasma, no detailed measurements of temperature fluctuations associated with drift waves have been made. This is a crucial measurement as $\phi_p = \phi_f + \frac{KT}{e} \ln \frac{v_e}{\alpha v_i}$. We have obtained detailed time and space resolved measurements of temperature fluctuations associated with a drift wave in our dense, collisional plasma by sampling, with a box car integrator, at controlled phase with respect to the wave, the current drawn by a Langmuir probe

as the probe bias and position are varied. The probe characteristic for increments of time along the wave period and at various spatial locations is then constructed. We find that the presence of substantial temperature fluctuations results in a large departure of the $\tilde{n} - \tilde{\phi}_f$ phase shift ($\sim 110^\circ$) from the $\tilde{n} - \tilde{\phi}_p$ phase shift ($\sim 45^\circ$). In addition, the $\tilde{n} - \tilde{\phi}_p$ phase shift has the density fluctuation leading the potential fluctuation as required. This is an extremely important result as it is this phase shift which governs the magnitude (and direction!) of the wave induced diffusion losses. We have compared our measured temperature, density, floating and plasma potential fluctuations with the values calculated from the theoretical expression give by Motley and Ellis⁵, generalized to include finite-beta. In addition, comparison was made with both isothermal and adiabatic theories (the limits of infinite and zero heat conductivity, respectively). The measured temperature fluctuations ($\sim 5-15\%$ and $\sim 5^\circ$ phase shift) are in best agreement with the adiabatic assumption. We therefore used this in our derivation of the theoretical dispersion relation. These results were presented at the 1974 Albuquerque APS meeting and are discussed by Tang.

We originally prepared a detailed report of this work for submittal to Plasma Physics. However, we felt that without a measurement of the associated plasma losses that the work was incomplete. We therefore decided to increase the scope of the paper by making the appropriate measurement. The wave induced radial losses are given by $j_r = \langle \tilde{n} \tilde{v}_r \rangle$ where \tilde{n} and \tilde{v}_r are respectively the density and radial velocity fluctuations associated with the instability and j_r the radial flux of plasma. In the present case the wave is primarily azimuthal and we have $j_r = \frac{c}{B_0} \langle \tilde{n} \tilde{E}_\theta \rangle$ or $j_r = \frac{c n k_\perp}{B_0} \langle \tilde{n} \tilde{\phi}_p \rangle$ where n is the azimuthal mode number and k_\perp the perpendicular mode number. It should be noted that since $\tilde{\phi}_p \neq \tilde{\phi}_f$ in our case that simple density-floating potential correlation measurements are inapplicable and sampled probe techniques as described

above are employed. We have also used our correlator, but always apply the proper correction to account for the observed temperature fluctuations. Using these methods, we have completed measurements of the wave-induced radial flux associated with both branches of the drift-Alfvén instability. The measured diffusion exceeds Bohm by better than a factor of two and is obviously a serious factor for equatorial spread F . This work was presented at the Florida APS Meeting. A paper describing the work has been accepted for publication in the Journal of Applied Physics.

B. Laser-Plasma Interaction Studies

We have begun an investigation into the problems involved in the development of a soft x-ray source using laser heating of plasmas. These schemes typically involve a high intensity CO_2 laser ($10.6 \mu\text{m}$) and either an underdense magnetically confined plasma or a critical density plasma such as the dense plasma focus. Our approach thus far has been to perform scaled experiments in the microwave region where well-diagnosed plasmas and high power rf sources are easily obtained.

Our first effort in this regard has been the study of the effects of a broadband rf pump field on the threshold growth rate and saturation level for the parametric decay instability. It has now been well documented that although the excitation of the parametric decay instability can result in substantial electron heating above threshold, a large fraction of the energy goes into the production of suprathermal electrons. This can have a devastating effect on both D-T pellet compression and on the heating of a target plasma for soft x-ray production. The use of a broadband pump is expected to increase the threshold for this dangerous instability.

The physical mechanism of instability control by means of a finite bandwidth pump is easily understood. Parametric instabilities of both the absorptive and reflective types are resonant interactions. This is illustrated by the upper sketch in Figure 1 which depicts the instability threshold power as a function of the center frequency for the case of a narrowband pump. The instability resonance width γ is indicated. The bottom sketch portrays the spectral power distribution of a typical wideband pump. As can be seen, only the power contained within the resonance width γ is available to excite the instability. Therefore, for the case of a randomly modulated pump whose energy is uniformly distributed over a bandwidth $\Delta\omega$ much larger than γ , the effective power available to excite the instability is related to the incident power P_0 by $P_{\text{eff}} = \left(\frac{\gamma}{\Delta\omega}\right)P_0$. In this large bandwidth limit ($\Delta\omega \gg \gamma$), the precise mechanism responsible for producing the finite bandwidth pump has been found to be rather unimportant in terms of the effects on threshold and growth rate.⁶⁻¹³

To date, there has been very little experimental investigation of the effects of finite bandwidth laser-plasma interactions with the exception of the experiment of Yamanaka et al.¹⁴ Contrary to theoretical predictions, they found increased heating efficiency for the broader bandwidth laser. However, this may have been due simply to a decrease in reflected power.

To investigate this important question of laser bandwidth control of instabilities, we began a microwave experimental simulation of the interactions of a finite bandwidth driven pump with a plasma. A detailed discussion of our present results is contained in Sec. IIIB¹⁻³ together with our proposed extensions of this work. However, let us briefly summarize. Using a gridded parallel-plate

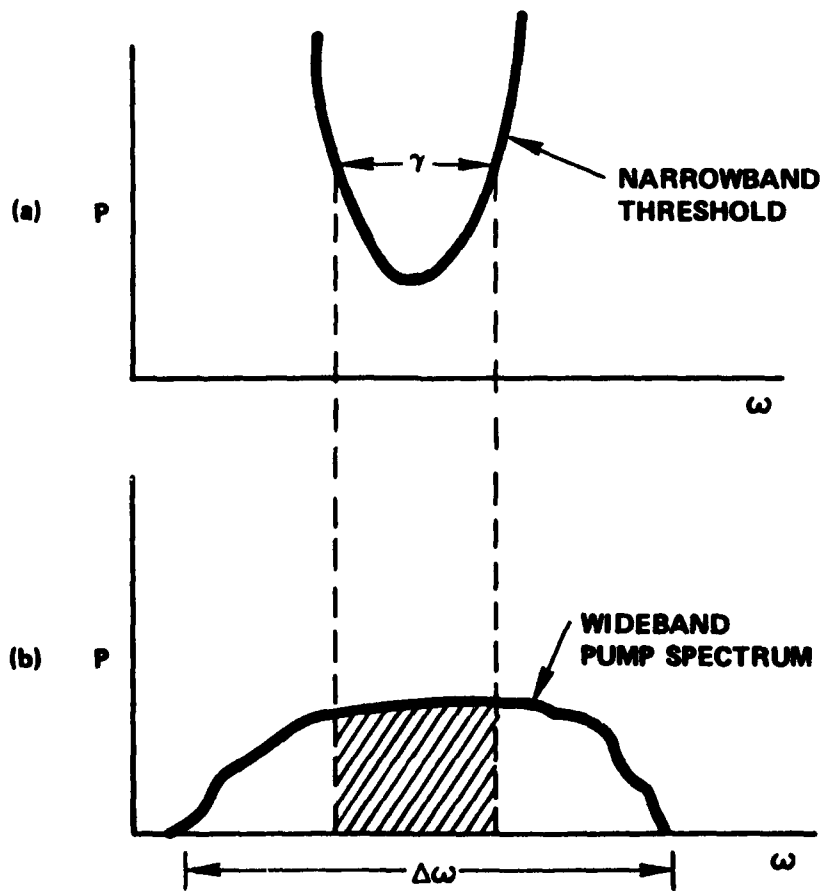


Figure 1. Illustration of Finite Bandwidth Pump Control of Parametric Instabilities. (a) The narrowband threshold curve is indicated as a function of pump center frequency. (b) The power spectrum of a broadband pump is shown with the "effective" power indicated by the cross-hatched region.

geometry similar to that of Stenzel and Wong¹⁵ we have verified that the use of finite bandwidth results in increased thresholds and decreased growth rates in agreement with theory.⁶⁻¹³ This work¹⁶ has recently been accepted for publication in Phys. Rev. Lett. and is contained in Appendix A. More recently,¹⁷ we have employed higher power and a gridded microwave horn for wave launching to verify that finite bandwidth can reduce the population of instability produced hot electrons.

As discussed above, we have performed two separate experiments (1) a low power experiment to determine the effects of a finite bandwidth pump on the instability threshold and growth rate, and (2) a high power experiment to investigate the effects of finite bandwidth on electron tail heating. This will be discussed in Sec. IIIB.2 and Sec. IIIB.3, respectively. In Sec. IIIB.1, we will briefly mention the various methods used to generate the wideband pumps as the characterization of the noise is of great importance in comparison with theory.

1. Finite Bandwidth Pump Production

Since our aim was to compare our results with existing theory wherever possible and also to provide the means for future comparison with theory, great care was taken with the wideband pump source so that the noise was well characterized. The sources were capable of steady-state operation for the lower power threshold experiments, but could also be pulsed with a risetime < 20 nsec to facilitate the measurement of growth rates.

The simplest method of producing wideband noise, and the one which has yielded the largest bandwidth, employs a doubly-balanced mixer in which the output of a variable-width ($\Delta\omega_n$) Gaussian white noise generator was mixed with a coherent high frequency signal producing an rf output of bandwidth $\Delta\omega = 2\Delta\omega_n$

which was subsequently amplified to the desired power level. The resulting 100% random amplitude modulation produces noise pumps with widths $\frac{\Delta\omega}{\omega_0}$ up to $\sim 40\%$.

In Figure 2 we have shown spectrum analyzer traces of typical noise pumps produced by this technique. The top trace corresponds to a 40 MHz wide noise pump $\left(\frac{\Delta\omega}{\omega_0} \approx 2\%\right)$. Note that the spectral power distribution is nearly constant over the full width of the pump. The bottom trace corresponds to a considerably broader pump with a width of about 320 MHz $\left(\frac{\Delta\omega}{\omega_0} \approx 13\%\right)$. Again, the power distribution is observed to be relatively flat.

An alternate method involves helix-modulation of a traveling wave tube (TWT) amplifier with a voltage waveform of the desired type. In this fashion, we are able to produce wide-bandwidth, phase modulated pumps with less than 5% attendant amplitude modulation. The resulting RF field is given by $E(t) = E_0 \cos(\omega_0 t + \alpha(t))$ where $\alpha(t)$ is the particular phase modulation. To generate well-characterized noise phase modulation, we have employed Gaussian white noise of adjustable amplitude. It is also of interest to examine the effects of a coherent sinusoidally phase modulated pump on the parametric instability. In this case $\alpha(t) = x \cos(\omega_m t)$ where x is the modulation index and ω_m is the modulation frequency. The rf field may then be expanded in terms of Bessel functions and its Fourier spectrum consists of sidebands of amplitude $J_n(x)$ and frequency $\omega = \omega_0 \pm n\omega_m$. Therefore, if $\omega_m \gg \gamma$ the instability resonance width, the effective power contained within γ is simply $P_{\text{eff}} = P_0 J_0^2(x)$. We will make use of this relationship in Sec. IIIB.2.

The pumps described thus far are completely characterized, and therefore permit the unambiguous comparison with theory. We have also employed additional noise pumps whose noise is not so completely characterized. One such system employed an IMPATT (Impact Ionization Avalanche Transit Time) diode, a p-n junction reverse-biased to operate in the avalanche-breakdown regime. Mounted

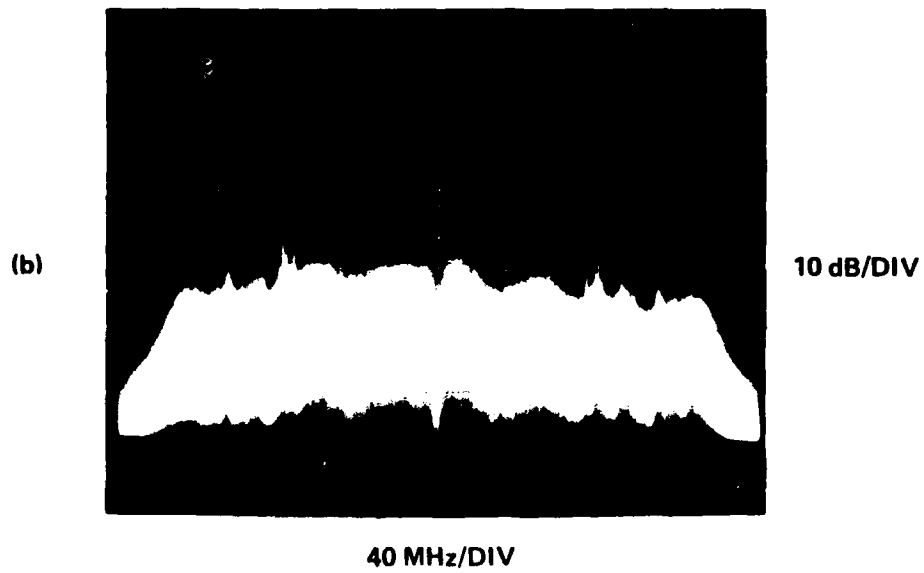
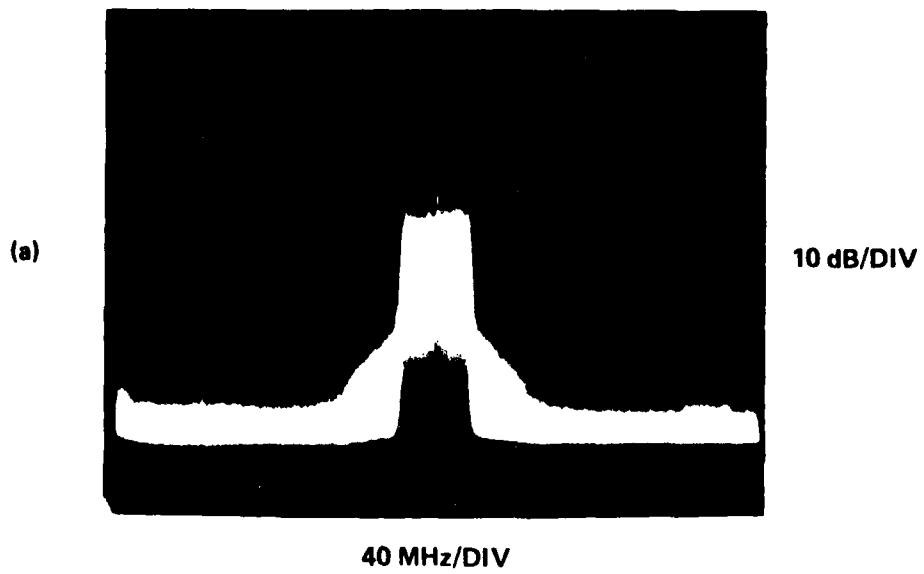


Figure 2. Typical Doubly-Balanced Mixer Produced Noise Pumps. Pump Center Frequencies were 2.5 GHz.

in a properly tuned waveguide, this solid state source is capable of producing narrow band RF power of 500mW at 10GHz in the x-band. By detuning its cavity, however, it is possible to turn this into a variable bandwidth noise source, producing 0.1 mW in a range of frequencies up to several hundred MHz wide around 10GHz. For the 3cm wavelength experiments, this noise can be directly amplified to the desired power levels.

For the lower plasma densities corresponding to plasma frequencies near 1 GHz, for example, the signal from the wideband IMPATT source is mixed with the signal from a stable, single-frequency x-band oscillator around 9 GHz. Hence, the down-converted noise spectrum is centered around the desired 1 GHz, and may, in turn, be amplified to the required power levels.

2. Effect of Finite Pump Bandwidth on the Parametric Decay Instabilities.

In this section we describe our experimental investigation of the effect of finite pump bandwidth on the parametric decay instability. Figure 1 illustrates the mechanism for control of parametric instabilities using a finite bandwidth pump. Figure 1(a) indicates the variation in threshold power for parametric instability as a function of the frequency of a narrow band pump. The resonance width may be characterized by the quantity γ . The power spectrum for a finite bandwidth pump is sketched in Fig. 1(b). Theory⁶⁻¹³ predicts that the pump power available to drive the instability is that contained within the resonance width γ . This fraction of the total power is illustrated by the cross-hatching on the lower graph. For $\Delta\omega \gg \gamma$, the broadband threshold power P_{th} is related to the narrowband threshold P_{th}^{NB} by $P_{th} = \frac{\Delta\omega}{\gamma} P_{th}^{NB}$.

We have experimentally examined the effects of finite bandwidth on the parametric decay instability. Figure 3 depicts schematically the experimental apparatus used in this investigation. The plasma is produced by a hot cathode discharge in argon and employs electrostatic confinement of the electrons.

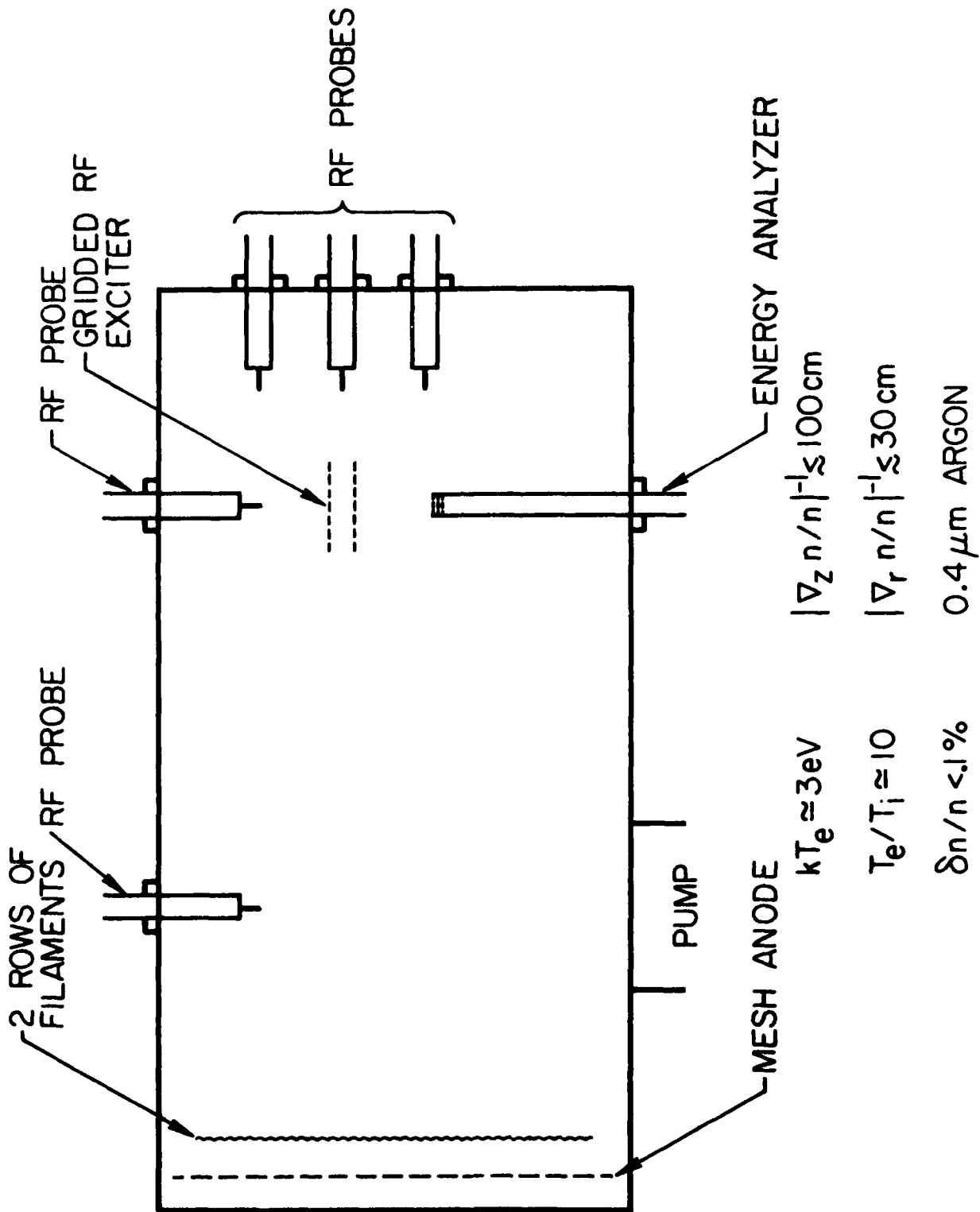


Figure 3. Schematic of Experimental Apparatus used to Investigate the Effects of a Finite Bandwidth Pump on the Parametric Decay Instability.

The design is based on a similar plasma source developed at the University of California at Davis.¹⁸ A uniform, unmagnetized plasma is produced within the chamber. Typical plasma parameters for our experiments were densities $n_e \approx 10^{10} \text{ cm}^{-3}$, electron temperature $T_e \approx 3\text{eV}$ and electron ion temperature ratios $T_e/T_i \approx 8-10$. This large electron-ion temperature ratio facilitates excitation of the parametric decay instability. For this particular experiment the RF is applied to a set of highly transparent grids similar to those employed by Stenzel and Wong.¹⁵ Shielded single and double probes are used to detect the generated ion and electron waves.

When the pump frequency lies near the plasma frequency, we observe the parametric decay instability for pump powers above a well defined threshold value. Slightly above threshold, we observe a well-defined ion disturbance whose spectrum peaks around 400KHz and corresponding Langmuir waves whose frequency is displaced $\sim 400\text{KHz}$ below the pump frequencies. At higher pump powers, both the ion and Langmuir spectra become turbulent, the power spectrum extending over several hundred KHz. The evolution of the spectrum is shown in Figure 4 where spectrum analyzer traces of the high frequency decay waves are shown near threshold (upper trace) and at somewhat higher power (lower trace). Figure 5 shows the growth of the ion acoustic wave when the RF source is pulsed on. The upper trace is simply a reference pulse which indicates when the RF power is nonzero. The lower oscilloscope trace displays the output of a double probe located $\sim 3\text{cm}$ from the excitation grids. The finite time of propagation to the probe and persistence of the oscillations after the RF pump excitation ceases agree quantitatively with the computed ion acoustic velocity for our plasma.

The resonance width of the instability is determined by varying the frequency of a narrow-band pump and noting the threshold powers. Typically the resonance width, which we define as the full width between the twice power

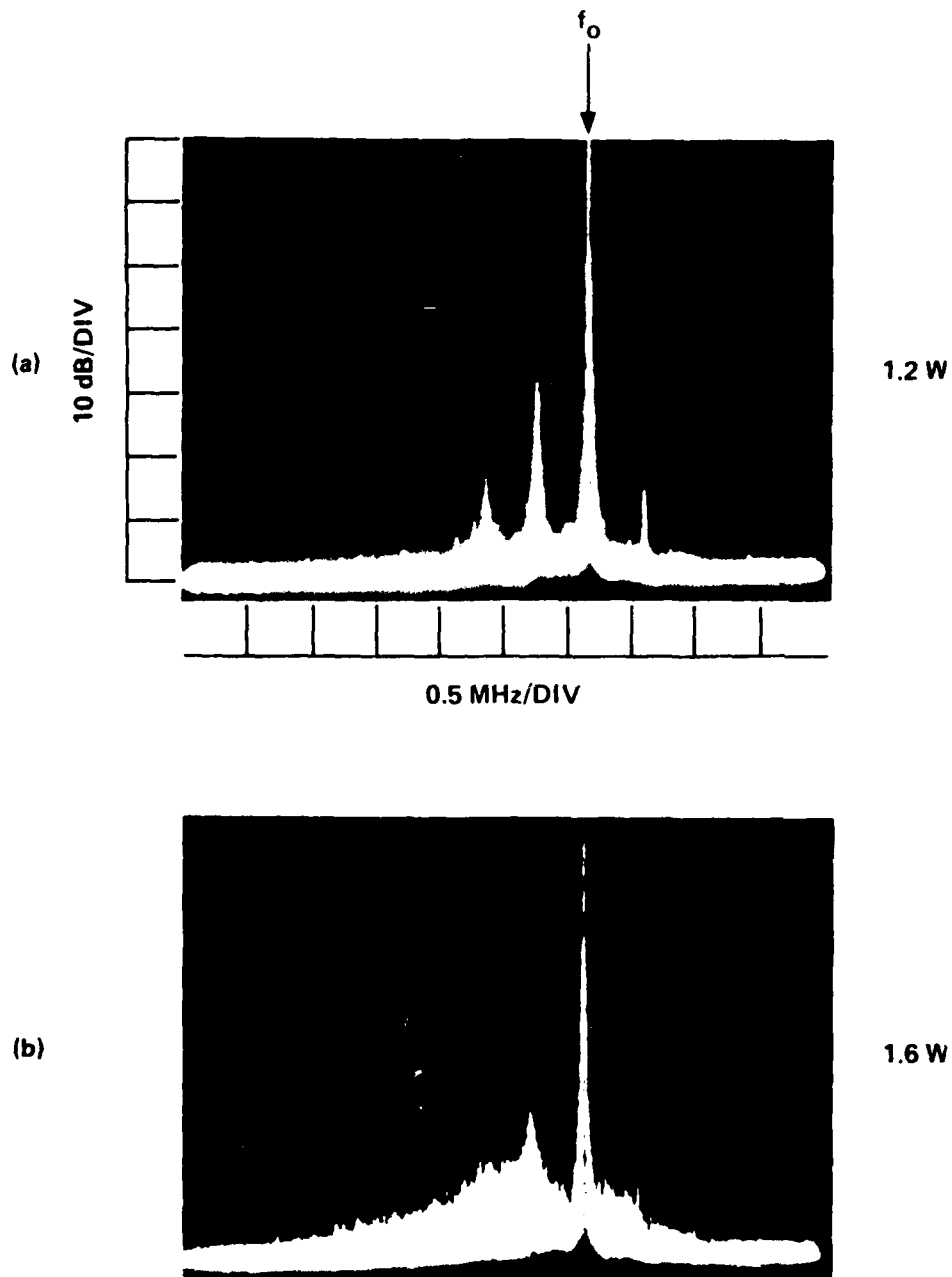


Figure 4. Spectrum Analyzer Traces of the High Frequency Decay Waves Produced by a Narrowband Pump.

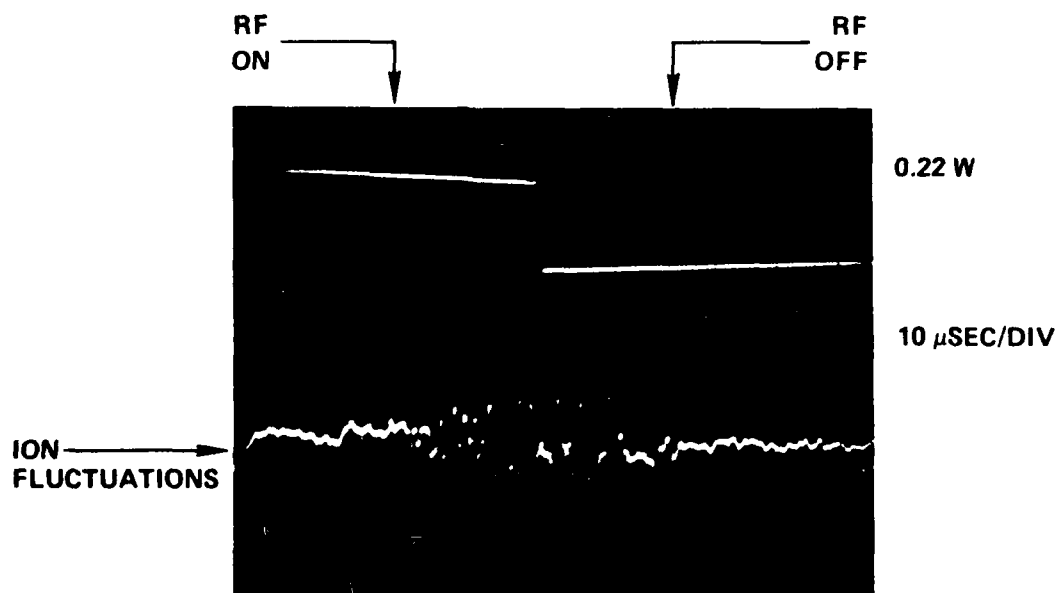


Figure 5. Time Evolution of Instability Produced Ion Waves Detected by a Double Probe.

points, is approximately 1% of the pump center frequency. This is larger than that calculated from uniform plasma theory, but is consistent with the boundary conditions, which include gentle density gradients due to the insertion of the excitation grids into the plasma, and the finite size interaction region.

Figure 6 displays the observed ion acoustic fluctuation level for both a narrow-band and a wide-band $\left(\frac{\Delta\omega}{\omega_0} \approx 4\%\right)$ pump. In each case, the pump center frequency was adjusted to coincide with the value for minimum threshold power. The ordinate in Figure 6 is the square of the average ion acoustic amplitude, while the abscissa is the pump power. Here the averaging is over the frequency range $0 < \omega_{\text{ion}} \lesssim \omega_{\text{pi}}$. A definite reduction in the saturated ion fluctuation level is observed for the case of the wide-band pump. The threshold for the narrowband pump is sharp, with the fluctuation level increasing rapidly to a value which only slowly increases upon further increase in pump power. The value of the wideband threshold power is both higher and less well defined than the narrowband case. Thus we see a pronounced effect when a wideband pump is employed. By varying both the plasma and pump parameters, we have been able to quantitatively compare this effect with that predicted by theory.⁶⁻¹³

Figure 4a shows the power spectrum for the wide-band pump used to obtain the results shown in Figure 6. This particular pump was produced by noise amplitude modulation of a monochromatic microwave signal as described in Sec. IIA.1. The pump bandwidth can be varied continuously from essentially zero to approximately 4% of the center frequency. In the limit that the pump bandwidth is large compared to the instability resonance width, theory predicts that the threshold power for the decay instability should increase linearly with the pump bandwidth.

The graph shown in Figure 7 displays the experimental threshold power required to obtain a given density fluctuation level plotted as a function of pump

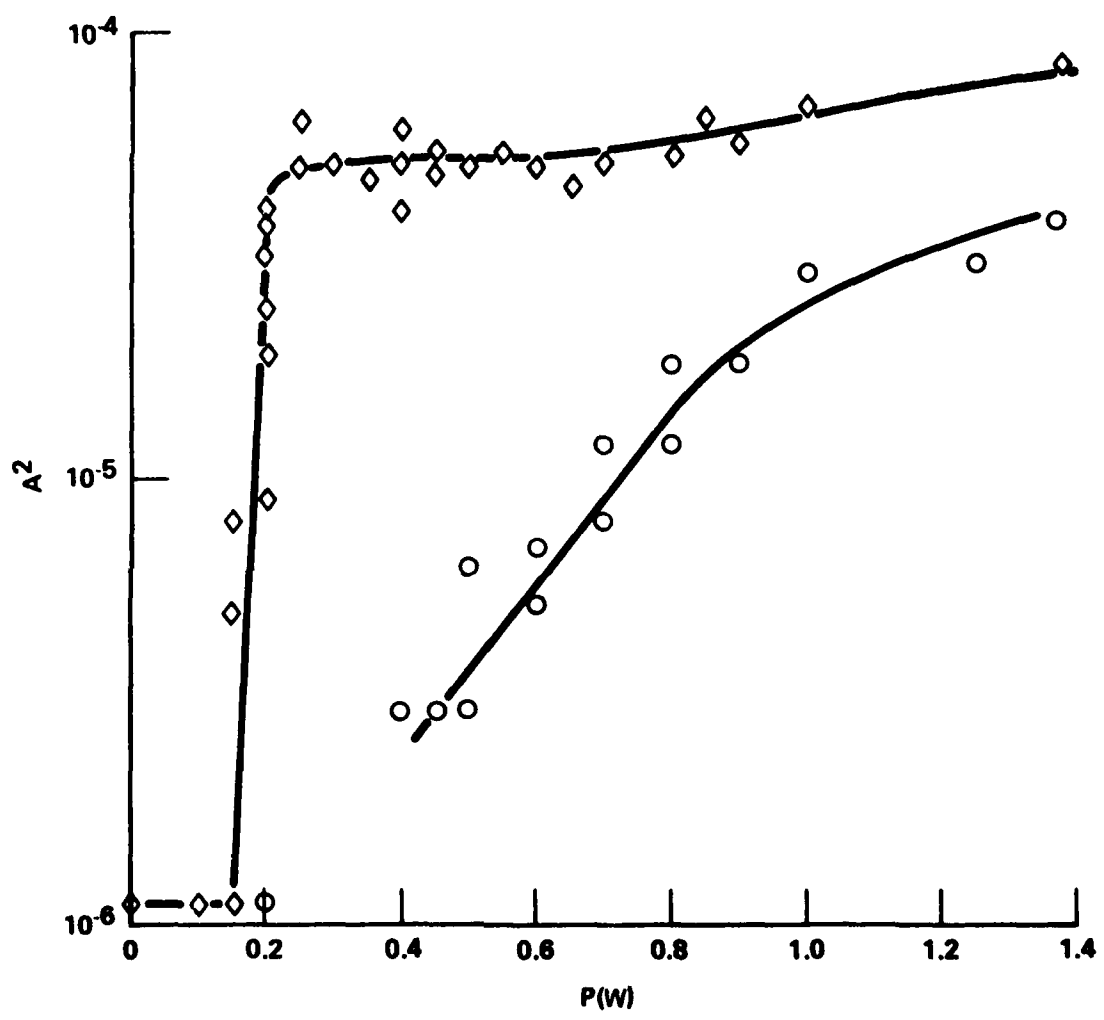


Figure 6. Saturated Ion Acoustic Fluctuation Level for a Narrowband Pump (\diamond) and a Broadband Pump (\circ) with Bandwidth $\Delta\omega/\omega_0 \approx 4\%$.

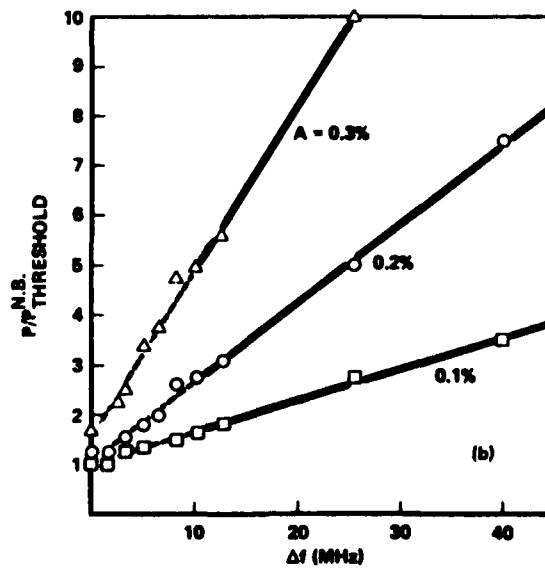


Figure 7. Pump Power (Normalized to the Narrowband Threshold) Required to Produce a Given Density Fluctuation Level A as a Function of the Width of the Balanced Mixer Produced Noise Pump.

bandwidth. The threshold for density fluctuations levels, $\frac{\Delta n}{n} = .1\%, .2\%$ and $.3\%$ are plotted. In each case, we obtain a linear relationship between the threshold power and pump bandwidth in agreement with theoretical predictions. From the slopes of the lines drawn through the experimental data points, one can calculate the instability resonance width, " γ ", necessary to obtain these results. In Table 1 we tabulate the values for γ obtained from the slopes in Figure 7 and compare these values with those obtained from scanning a narrow band pump through the instability resonance. There is seen to be reasonable agreement in the values for γ obtained by these two methods.

Table 1. Instability Resonance Width $\frac{\Delta\omega}{2\pi}$

Fluctuation Level	Resonance Width* (MHz)	Resonance Width [†] (MHz)
0.1%	25	16
0.2%	14	8
0.3%	8	6

* Resonance width determined using narrowband pump.

† Resonance width obtained from slopes in Figure 7.

We have also examined the effects of scanning the center frequency of various finite bandwidth pumps through the instability resonance. Figure 8 shows the ion acoustic fluctuation level for various values of pump power, plotted as a function of pump center frequency. Here we present the results of bandwidths ranging from essentially zero to 1.2%. Note that the reduction in the fluctuation level is a monotonic function of pump bandwidth and occurs for all pump center frequencies. It is interesting to note that the results displayed in Figure 8 were obtained with a noise phase modulated pump, while those shown in Figure 6 correspond to a noise amplitude modulated pump.

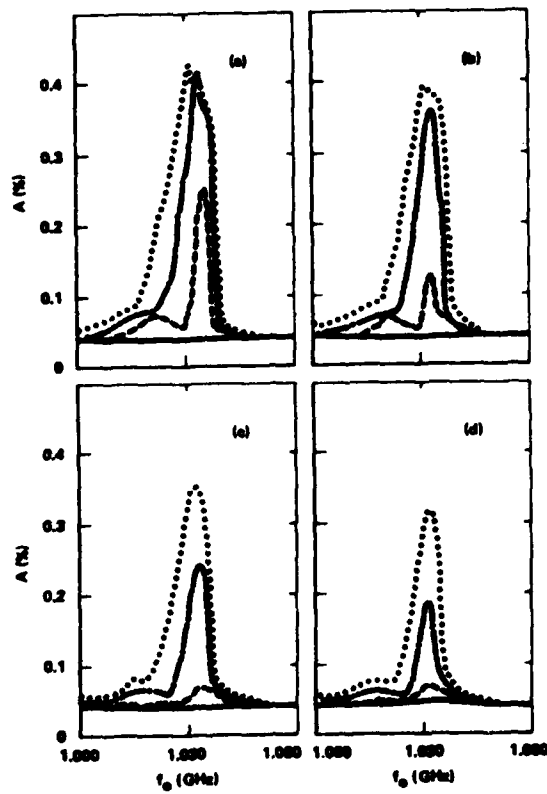


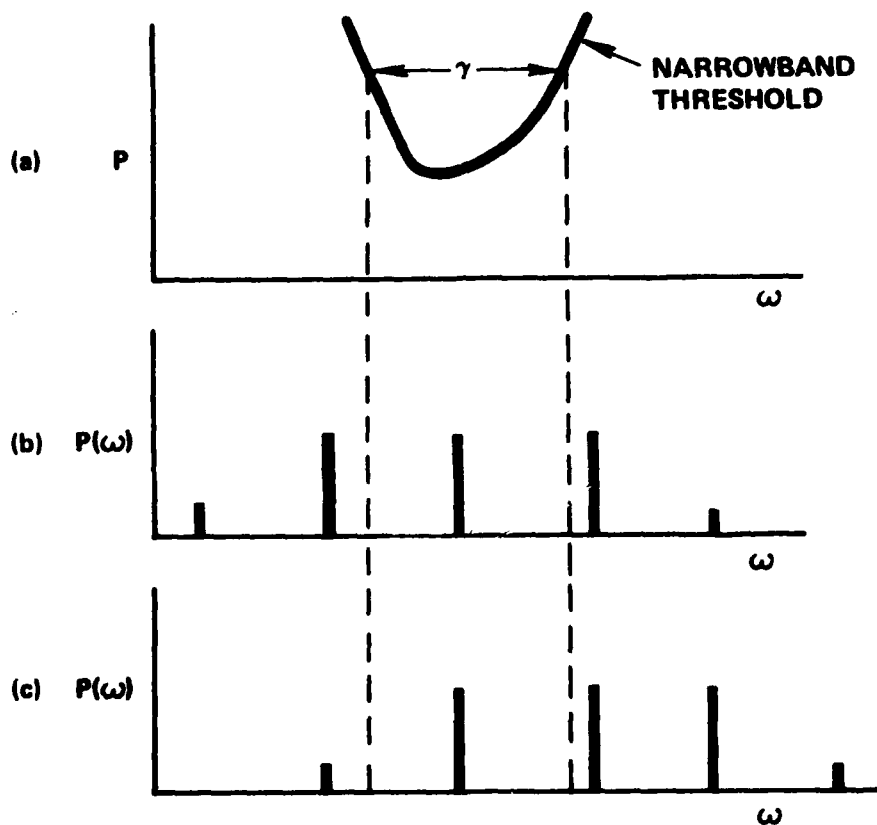
Figure 8. Saturated Density Fluctuation Level A as a Function of Pump Power and Center Frequency for the Noise Phase Modulated Pump. The noise bandwidth $\Delta\omega/2\pi$ is < 10 kHz for (a), 3 MHz for (b), 6 MHz for (c) and 12 MHz for (d). Pump power is varied from 0.5 to 2.0 W: — 0.5W, - - - 1.0W, - · - 1.5W and · · · · 2.0W.

The similarity of the results for amplitude and phase modulated pumps in the large bandwidth limit ($\Delta\omega \gg \gamma$), indicates that for noisy pumps with continuous power spectral distributions, the particular mechanism for the bandwidth is not important.

We also examined another broadband pump which has a discrete, rather than continuous, power distribution. As discussed in Sec. IIA.1, for the case of sinusoidal phase modulation, the RF field is given by $E(t) = E_0 \cos(\omega_0 t + x \sin \omega_m t)$, where ω_m is the modulation frequency and x the modulation index. The Fourier amplitude spectrum of the pump then consists of the fundamental with amplitude proportional to $J_0(x)$, and modulation sidebands of amplitude $J_n(x)$ and frequency $\omega = \omega_0 \pm n\omega_m$ where n is an integer. In Figure 9 we illustrate what could happen if one employs a sinusoidally phase modulated pump to excite a parametric instability. Figure 9(a) is again a plot of narrow band pump threshold as a function of the pump frequency. The center graph (Figure 9(b)) illustrates the case where the center frequency of a sinusoidally phase modulated pump is tuned to the resonance center. If the modulating frequency is larger than γ , theory predicts that only the power in the center lobe is available to excite the instability. Finally, Figure 9(c) illustrates what could occur if the pump center frequency is not tuned to resonance center, but one of the sidebands is.

In Figure 10 we present the experimental results where the center frequency of a sinusoidally phase modulated pump is tuned to resonance center, and the modulation frequency is larger than the resonance width. Here we plot the normalized threshold power as a function of the modulation index x . The power contained within the fundamental center lobe is proportional to $J_0^2(x)$. Therefore, theory predicts that the threshold power to be proportional to $1/J_0^2(x)$:

$$P_{\text{thres}}(x) = J_0^{-2}(x) P_{\text{thres}}(0)$$



**SINUSOIDAL PHASE MODULATION
INDEX = 1.4**

Figure 9. Illustration of the Effects of a Sinusoidally Phase Modulated Pump on the Parametric Instability. (a) Narrowband Threshold Power as a Function of Pump Frequency. (b) Fourier Spectrum of Sinusoidally Phase Modulated Pump with Center Frequency Coincident with Threshold Minimum (c) Modulation Sideband Coincident with Threshold Minimum.

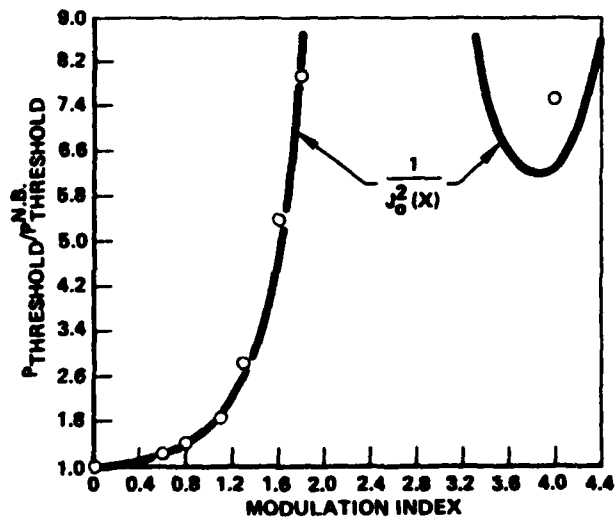


Figure 10. Threshold Power Normalized to the Narrowband Threshold as a Function of Modulation Index for a Sinusoidally Phase Modulated Pump ($\omega_m > \gamma$). Solid Curve is $J_0^2(X)$.

The solid line in Figure 9 is this theoretical result. Note the agreement between theory and experiment, including a point on the second cycle of the Bessel function. It should be stressed that there have been no points "fitted" for this plot. The solid curve is simply $J_0^{-2}(x)$ and the points are our experimental results.

We have also examined the results of sweeping the center frequency of a sine modulated pump through the instability resonance. In Figure 11, we display the saturated amplitude of the ion fluctuations as a function of pump center frequency for several power levels. Here the modulation frequency $\frac{\omega_m}{2\pi}$ is comparable to the instability resonance width γ . The modulation index is zero for Figure 11(a), i.e. the narrowband case, and increases in Figures 11(b-d). In Figures 11(c) and 11(d) where the modulation index is high, we see the apparent offset of the resonant frequency as the pump sidebands pass through the instability resonance.

In conclusion, our experiments with the decay instability employing gridded capacitor-plate wave launchers have shown good agreement with theory for pumps whose bandwidth is large compared with the resonance width. We see significant increases in thresholds and decreases in growth rates and saturated amplitude levels for the parametric decay instability when the wide pump is employed.

Our future experiments with this particular experimental geometry (where the RF is applied to capacitor grids) will center about two areas. First, we have recently obtained microwave sources of increased power output, and wider bandwidth pumps, which will allow us to investigate heating of the plasma, and to extend the results given in this section. We will also investigate in more detail, the effects of employing narrower bandwidth pumps. Our preliminary results indicate that complex phenomena occur when the pump bandwidth is smaller than the resonance width, yet comparable to the frequency of the ion acoustic

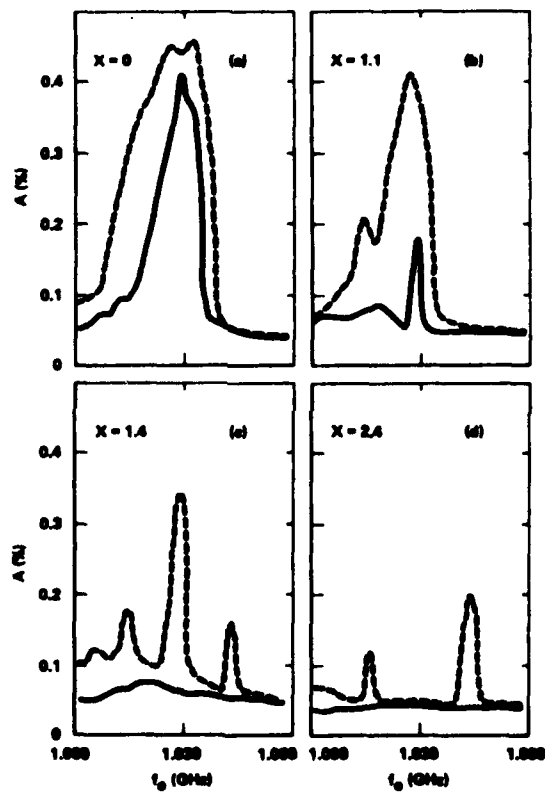


Figure 11. Saturated Density Fluctuation Level A as a Function of Pump Power and Center Frequency for the Sinusoidally Phase Modulated Pump ($\omega_m/2\pi = 14 \text{ MHz} > \gamma/2\pi$). The modulation index is $X = 0$ for (a), $X = 1.1$ for (b), $X = 1.4$ for (c) and $X = 2.4$ for (d). For $X = 1.4$ the pump power is distributed approximately equally between the center frequency and the first upper and lower modulation sidebands, while for $X = 2.4$ the power at the center frequency is approximately zero. Two values of pump power are shown: ——— 2.0W and - - - - - 4.0W.

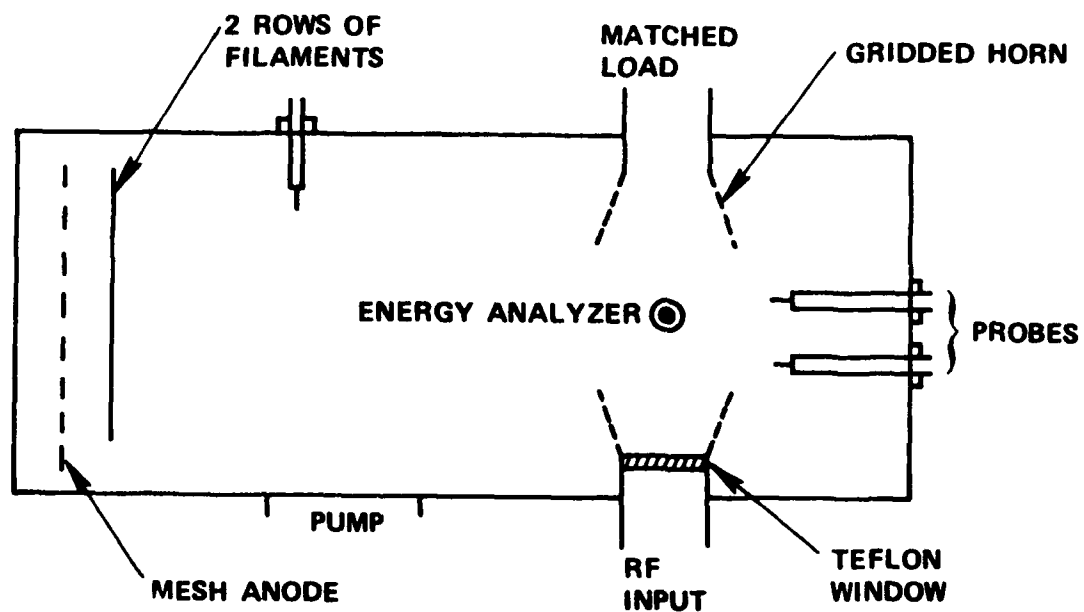
waves. Under these conditions, we have found definite differences among the various pump bandwidth mechanisms in regard to their effect on threshold. For example, we have observed slight reductions in threshold powers when a double pump is employed to excite the decay instability when the double-pump difference frequency is equal to the produced ion acoustic waves in apparent agreement with available theory.¹⁹ In contrast, we see no such resonance behavior when a sinusoidally phase modulated pump is employed and the modulating frequency is tuned to the ion acoustic frequency.

3. 10cm Finite Bandwidth Heating Experiment

As described in the previous section, we have verified the increase in thresholds and decrease in growth rate and saturation level for the parametric instability driven by a broadband pump. A gridded capacitor plate geometry similar to that of Stenzel and Wong¹⁵ was used to launch the pump.

We have recently begun an experiment which employs a different geometry. The purpose of this experiment was two-fold: one was to demonstrate that our previous agreement with theory was not restricted to the particular geometry employed. The second purpose was to use higher power and to investigate the effects of finite bandwidth on heating -- especially electron tail heating. Preliminary results of this experiment are discussed in this section.

The experimental apparatus is shown schematically in Figure 12. The unmagnetized plasma is produced by a filament-discharge with electrostatic confinement of the primary electrons. The pump frequencies are typically 3GHz in this case. Therefore, to obtain the required 10^{11} cm^{-3} plasma density, the plasma is pulsed rather than steady-state as in the previous work. Plasmas are produced with density $n_e \leq 5 \times 10^{11} \text{ cm}^{-3}$, electron temperature $KT_e \approx 2.5 \text{ eV}$, and temperature ratio $T_e/T_i \approx 8-10$. The pulsed discharge is produced by the discharge of a capacitor bank using a silicon controlled rectifier (SCR).



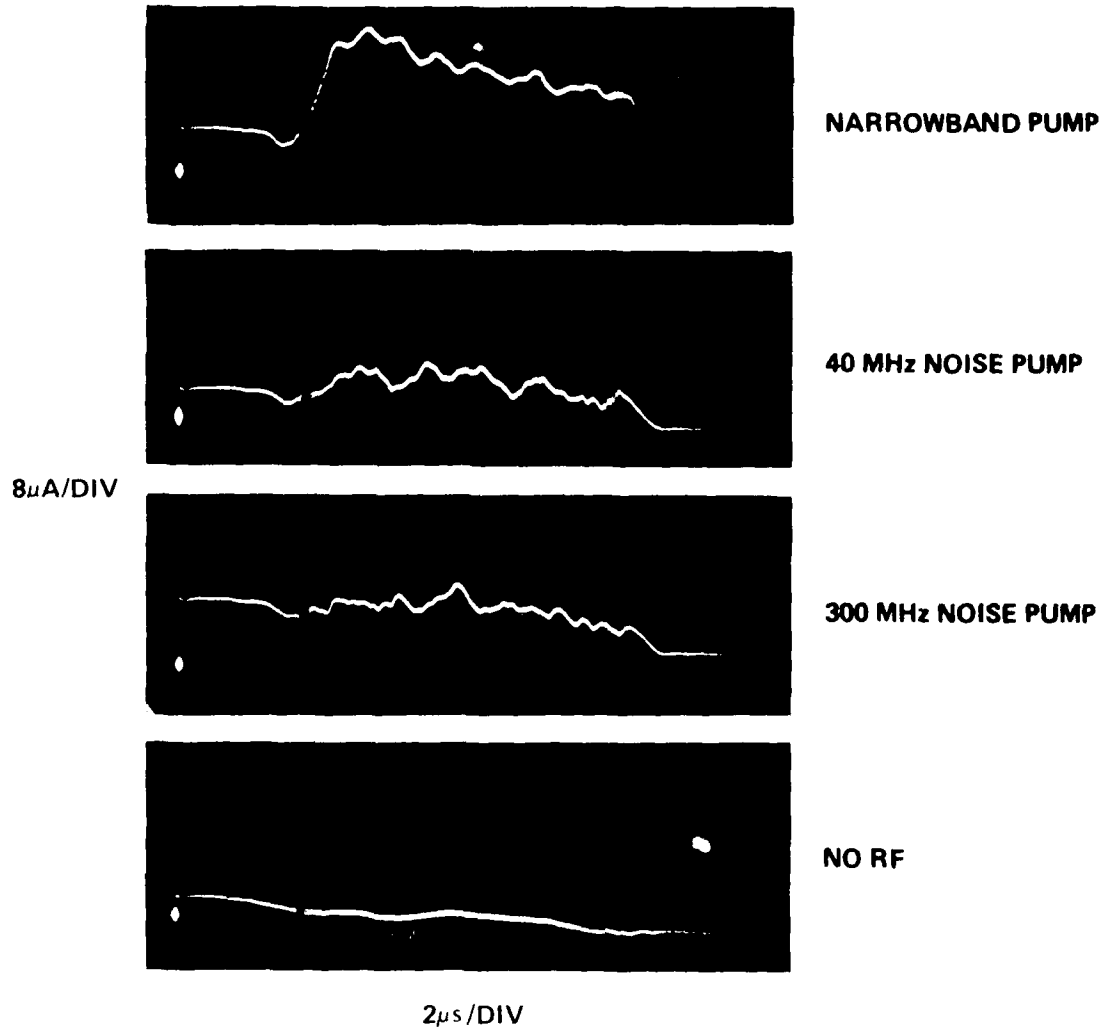
$n_e > 10^{11} \text{ cm}^{-3}$ $KTe \approx 3 \text{ eV}$
 0.4 μm ARGON

Figure 12. Schematic of Experimental Apparatus Employed to Determine the Effect of Finite Pump Bandwidth on Electron Tail Heating.

Using a fast swept (1 μ s) Langmuir probe, the temporal behavior of the plasma density and temperature are obtained. The FWHM of the plasma density is about 4msec. Since we are interested in the parametric decay instability, which is a resonant interaction, it is important for the plasma frequency to be relatively constant over the duration of the RF heating pulse. For the typical pulse lengths of 10 μ s used in these heating measurements, the change in plasma frequency is only about 0.1%. This shift is small compared to the 1-16% bandwidth of the noise pumps employed.

As indicated in Figure 12, the RF excitation is electrodeless and consists of a gridded RF horn to launch the pump. The measured plasma density increases by about a factor of five in one free space wavelength from the teflon window and then is relatively constant across the chamber (falling to zero, of course, at the opposite wall). The particular type of noise employed in these heating measurements was random amplitude modulation produced with a doubly balanced mixer as described in Sec. IIIB.1. The multigrid electrostatic energy analyzer shown in Figure 12 detects fast electrons excited along the direction of the pump electric field.

The use of finite pump bandwidth is found to significantly reduce the population of instability produced hot electrons as indicated by Figure 13. In this figure, oscilloscope traces are displayed of the hot electron current measured with the retarding grid electrostatic energy analyzer. The average RF power level corresponding to the three upper traces was held constant at about 320W which is well above instability threshold. The analyzer was biased to accept all electrons with energy greater than 45 eV or about 17 times the thermal energy. As can be clearly seen, the use of finite bandwidth reduces the detected hot electron current. The 40MHz pump is identical to the one shown in Figure 2(a). However the "300MHz" pump used here was not as flat as the one displayed in



ANALYZER ELECTRON CURRENT ($U < -45V$)
 $P = 320 W, f_0 = 3.05 GHz$

Figure 13. Energy Analyzer Measurements of the Effects of Finite Pump Bandwidth on the Production of Hot Electrons.

Figure 2(b) and actually had an effective width of more nearly 100MHz, which accounts for the very slight difference between the middle traces in Figure 13. The noise level shown in the bottom trace was reduced in subsequent work so that hot electron heating rates could also be measured.

Figure 14 displays the saturated hot electron current as a function of pump power with the pump center frequency held constant at a frequency corresponding to minimum threshold. Electrons with energy greater than 150 eV or about 58 times thermal energy are accepted by the analyzer. The upper trace corresponds to a narrowband pump while the lower curve results from the noise pump with an effective width of ~ 100 MHz. The saturated hot electron current is seen to be reduced by finite bandwidth at all power levels.

We have also determined the effects of finite bandwidth on the hot electron heating rate which we define as the initial time derivative of the hot electron current. Figure 15 shows the heating rate as a function of pump power for a narrowband pump (top curve) and the 40MHz noise pump (bottom trace). It should be noted that the initial heating rates are essentially linear in both cases. While it is tempting to claim agreement with theoretical predictions for the instability heating rate,²⁰ it must be stressed that there are other possible explanations for the observed heating rate. For example, it may arise in part due to the partial confinement of some of the hot electrons by the electrostatic confinement. However, the important point is that the heating rate is clearly reduced for the case of the finite bandwidth pump.

The temperature of the hot electron tail was measured with the electrostatic energy analyzer and in the case of the narrowband pump found to be ~ 112 eV or about 43 times the thermal energy. The reduction in the hot electron population was so large in the case of the wideband pump that it was difficult to obtain an accurate determination of the tail temperature for comparison. Such a measurement is of obvious importance and is part of the proposed program.

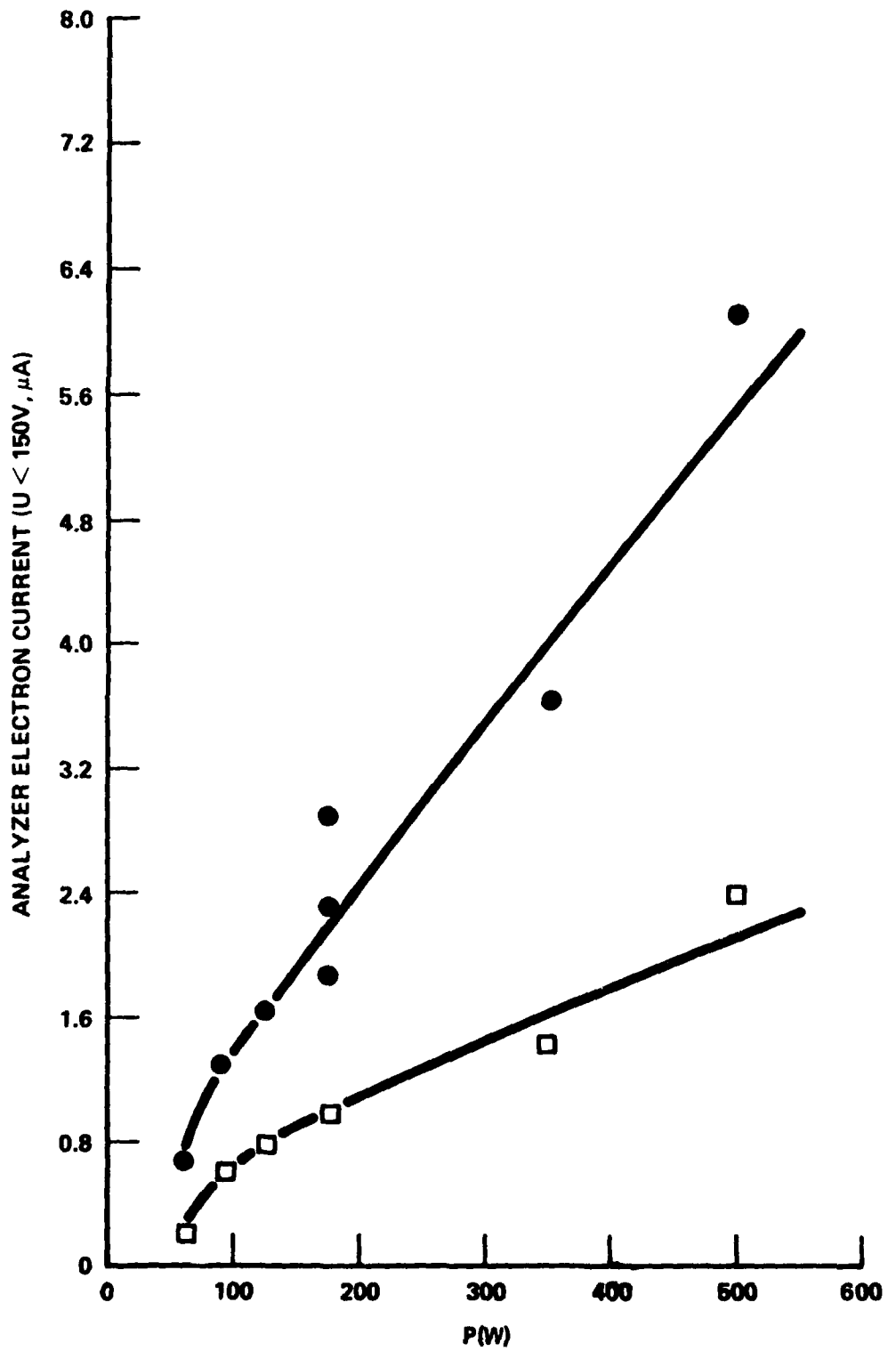


Figure 14. Energy Analyzer Electron Current as a Function of Pump Power for a Narrowband Pump (●) and the "300" MHz Pump (□). Curves show total particle currents collected above cut-off energy indicated.

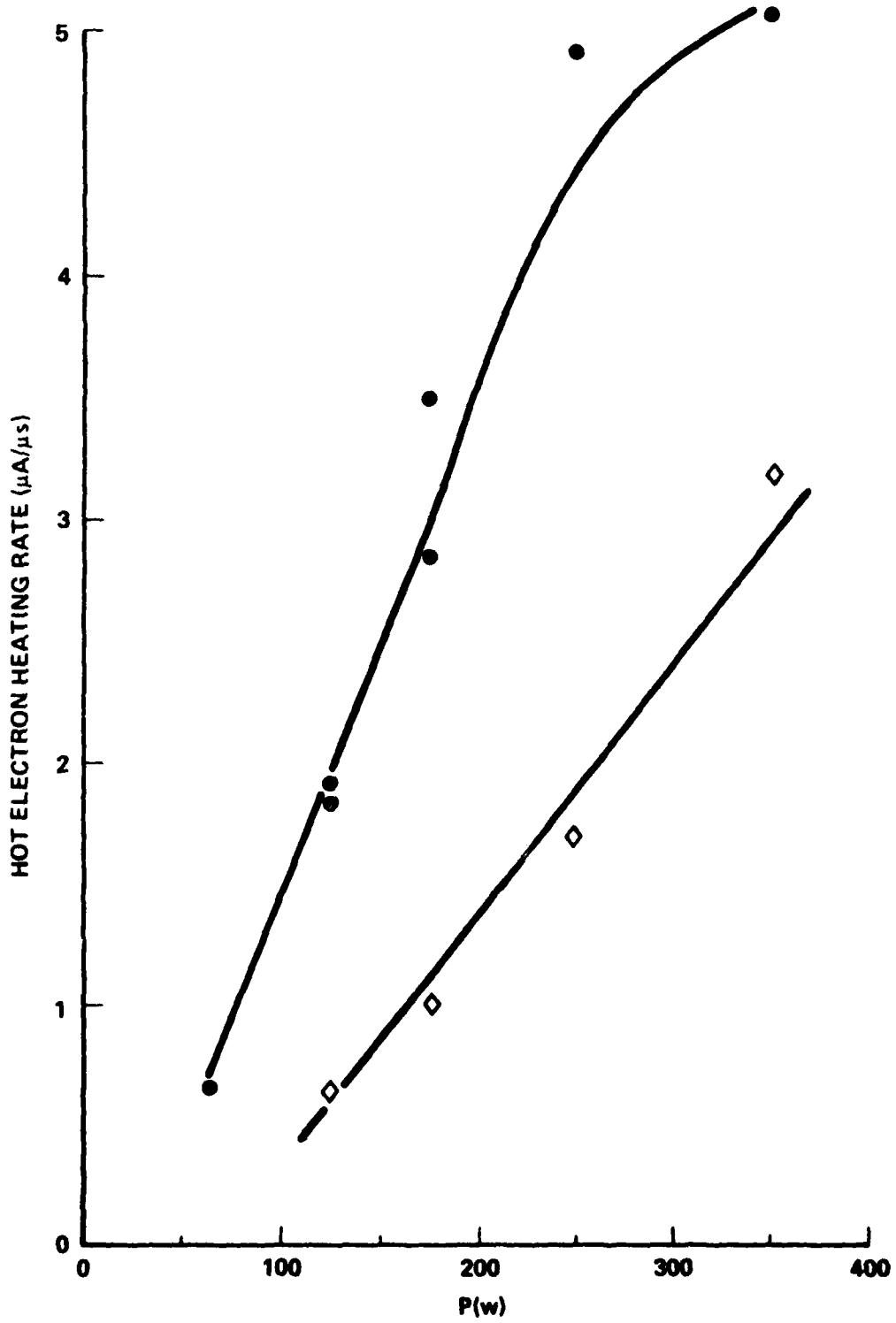


Figure 15. Hot Electron Heating Rate as a Function of Pump Power for a Narrowband Pump (●) and the 40 MHz Noise Pump (◇) Shown in Figure 2(a).

C. Current - Driven Electromagnetic Ion Cyclotron Instability

We have begun an investigation into the nature of a spontaneously occurring hydromagnetic instability with frequency near or below the ion cyclotron frequency and its harmonics. Our theoretical and experimental work has led us to believe that this instability is driven by the current in the arc region of our arcjet device. In this case the currents provide a source of free energy and thereby give rise to the instability. This instability has particular relevance to our AFOSR work on high beta instabilities since field-aligned currents between the ionosphere and magnetosphere are thought to destabilize certain waves and lead to "anomalous" resistivity.²¹ It should be noted that the work of Kindel and Kennel²¹ on topside current instabilities only treated the case of electrostatic ion cyclotron waves. Our efforts have therefore been divided equally between a theoretical derivation of the appropriate dispersion relations and further experimental work.

1. Theory

Since the only work that has been done concerning current-driven electromagnetic ion cyclotron (EMIC) instabilities has been the brief cold plasma treatment of CHATURVEDI and KAW²², we have therefore begun efforts to obtain the complete electromagnetic dispersion relation for our finite beta, current-carrying, collisional plasma. Our preliminary work has been completed and a first paper has been accepted for publication in Plasma Physics. In addition, the results of this theoretical study were presented at the Florida APS Meeting.

We have first derived the complete electromagnetic dispersion relation treating both the ion and electron components as fluids. The only further assumptions employed in the analysis were that the electron inertia could be ignored together with the parallel ion motion and displacement current. In addition, a simple isothermal equation of state was employed; the extension

to the adiabatic case is simple and the treatment of finite heat conductivity proceeds in a straightforward albeit tedious fashion. Both the collisional and collisionless contributions to the ion viscosity are included correctly to first order in b , where b is the finite Larmor radius parameter. Density gradient effects are ignored in our simple theory. The dispersion relation is solved under the assumption that $E_y = 0$, an approximation which facilitates solution and also appears to be justified by our experimental observations. In the limit $(\omega - k_z v_d) v_{ei} \ll k_z^2 v_{te}^2$ the real and imaginary parts of the wave frequency are given respectively by

$$x = k_z v_A \left(1 + \frac{k_x^2 v_s^2}{\Omega_{ci}^2} \right)$$

and

$$y = \frac{-v_{ei} k_x^2 v_s^2}{2\Omega_{ce} \Omega_{ci}} \left(1 - \frac{k_z v_d}{x} + \frac{b v_{ii} k_z^2 c^2 \Omega_{ce}^2}{2v_{ei} k_x^2 v_s^2 \omega_{pe}^2} \right)$$

where k_z (k_x) is the parallel (perpendicular) wavenumber, v_d the field-aligned electron drift velocity, ω the complex wave frequency, v_{te} the electron thermal velocity, Ω_{ci} (Ω_{ce}) the ion (electron) cyclotron frequency, v_{ei} (v_{ii}) the electron-ion (ion-ion) collision frequency, v_A (v_s) the Alfvén (sound) speed and ω_{pe} the electron plasma frequency. It is noted that both finite collision frequency and electron drift are required for instability and also that ion viscosity is stabilizing. Unstable waves with $\omega \lesssim \Omega_{ci}$ are therefore found to

occur when the electron drift speed becomes comparable to the Alfvén speed.

A brief comparison with our observed instability using our measured plasma parameters indicates that our model can provide the proper frequencies, wavenumbers and critical drift velocities.

The fluid picture can obviously not explain the observed higher harmonics. We have therefore undertaken to improve our model. Our first step has been to include kinetic effects by describing the ions through the Vlasov equation. For simplicity the electrons have thus far been treated as a cold fluid. The dispersion relation is then given by

$$-k_z^2 \frac{i\omega \omega_{pe}^2}{c^2 v_{ei} (\omega - k_z v_d)} - k_x^2 \frac{\omega_{pi}^2}{c^2 b k_z v_{ti}} \sum_{n=-\infty}^{\infty} n^2 \Gamma_n Z_n$$

$$+ \frac{i\omega_{pi}^2 \omega_{pe}^2}{c^2 b k_z v_{ti} c^2 v_{ei} (\omega - k_z v_d)} \sum_{n=-\infty}^{\infty} n^2 \Gamma_n Z_n = 0$$

where $\Gamma_n(b) = \exp(-b) I_n(b)$,

I_n = modified Bessel function of order n ,

$Z(\alpha_{in})$ is plasma dispersion function (FRIED and CONTE)

$$\text{and } \alpha_{in} = \frac{\omega + n\Omega_{ci}}{k_z v_{ti}}$$

For ion cyclotron waves $\alpha_{in} \gg 1$ and this has been solved for the growth rate retaining only the $n = \pm 1$ terms. The result is:

$$y = \frac{\Gamma_1}{b(K_x^2 + \frac{m_e}{m_i})} \left[-K_x^2 \frac{m_e}{m_i} v_{ei} \left(1 - \frac{k_z v_d}{x}\right) + (x^2 - \Omega_{ci}^2) \frac{m_e}{m_i} \frac{\pi^{1/2} e^{-\alpha^2}}{|k_z| v_{ti}} \right]$$

$$\text{with } K_x = \frac{ck_x}{\omega_{pe}} \quad \text{and} \quad K_y = \frac{ck_y}{\omega_{pe}}$$

To first order in b , $\frac{\Gamma_1}{b} \approx (1-b)$, it can be seen above that ion temperature and kinetic effects reduce the growth rate of the lowest order mode. We are now in the process of solving for the higher order modes. An extension to electron kinetic effects will be made using kinetic equation including a collision operator. Numerical solution of the resulting dispersion relations will be undertaken in order to facilitate comparison with our observed instability.

2. Experiment

The measurements and identification of a spontaneously occurring hydro-magnetic instability at or below the ion cyclotron frequency and harmonics have been continued. The frequency of the fundamental has been observed to be as low as $\Omega_{ci}/2$. Both discrete and continuous mode structure occurs with the discrete structure generally dominating at the lowest orders. The lowest order mode has been found to have azimuthal mode number $m=1$ using arrays of electric and magnetic probes. These results have also been verified by spectroscopic observations of the HeII 4686 Å line detected by an optical probe which can be scanned across the plasma column. The wave is a body wave (i.e. distributed throughout the plasma) with amplitude which decreases monotonically from the plasma column interior (of course vanishing exactly at the center as an $m=1$ should). At present, we have measured the axial and perpendicular wavelength using a boxcar integrator triggered by a reference probe. The input and triggering signals are passed through a band-pass filter to eliminate spurious signals. Probes are biased to collect ion saturation current and radially movable probes at several azimuthal locations are employed together with an axially movable probe whose radial position can be altered. The perpendicular wave number k_{\perp} is found to be given approximately by the inverse of the column radius. We find that $k_{\perp} \gg k_{\parallel}$, although a better determination must yet be made. Measurements using shielded magnetic pick-up loops indicate that $\tilde{B}_{\theta} \gg \tilde{B}_z > \tilde{B}_r$.

which can be shown to be well satisfied by our theoretical assumptions.

The measured instability frequency is found to be approximately proportional to the confining magnetic field B_0 in agreement with theoretical predictions. However, the intercept is nonzero. The width of the instability Δf is seen to be a minimum at 3 which can be explained by the theory. The instability frequency is also found to be a decreasing function of density. We have held the confining magnetic field constant in this case and varied the density. Finally, the frequency variation of the instability was found to be proportional to the square root of the electron temperature.

It is interesting to compare our results with the theoretical predictions. For purposes of comparison with our theory, we will pick the fundamental for one particular case: $n_e \approx 3 \times 10^{13} \text{ cm}^{-3}$, $T_e \approx T_i \approx 3 \text{ eV}$, $I_{\text{arc}} = 350 \text{ A}$, $B_0 = 2.5 \text{ kG}$, $k \approx 4 \text{ cm}^{-1}$, $k_{\parallel} \approx 0.065 \text{ cm}^{-1}$ and $f_{\text{instability}} = 450 \text{ kHz}$. Here the plasma parameters were measured in the experimental chamber where the density is approximately an order of magnitude lower than that in the arc region. Using the above experimental parameters, the predicted value of the instability frequency is 595 kHz. If we neglect ion viscosity, theory predicts marginal stability for $V_D \approx V_A$. This can be satisfied if we assume a uniform current distribution and use the density in the arc region to calculate V_D . However, if we include ion viscosity, the critical drift velocity is increased to approximately $4 V_A$. This can only be satisfied in the arc region if we postulate a nonuniform current distribution. This comparison is obviously of a very preliminary nature and concrete instability identification awaits thorough investigation of parameter dependence. However, it does not seem unreasonable that our present theoretical picture may turn out to correctly explain the observed behavior. This experimental work was presented at the May IEEE International Conference on Plasma Science held in Texas.

D. Nonlinear Evolution and "Anomalous" Resistivity

Of great importance is the mechanism(s) leading to the nonlinear saturated state of an instability, including the nonlinear frequency shifts, amplitude changes, etc. In addition, any increase in plasma resistivity beyond classical (i.e. "anomalous") has an important bearing on both the magnetospheric and ionospheric plasmas. To this end, we have begun an investigation into the saturated properties of the instability observed in the arcjet far beyond the current threshold and have also constructed a 1 kJ SCR-switched capacitor bank so that growth rates can be measured by large currents. We have made extensive studies of the plasma column I-V characteristic as a function of density and confining magnetic field strength. Strong indications of current-produced "anomalous" resistivity is observed. For example at a density of $5 \times 10^{14} \text{ cm}^{-3}$ and a confining magnetic field strength of 2 kG, the plasma resistivity increases by a factor of 6 when the column voltage is increased beyond 40V. The largest resistivity is obtained for intermediate values of magnetic field strength. Our aim is to positively identify the mechanisms and modes responsible for the increased resistivity.

E. Plasma Source Development

1. Arcjet Plasma

Our efforts in this direction were primarily concerned with completion of a series of detailed measurements of the plasma properties (density, electron and ion temperatures, etc.) obtained with the 0.75 cm diameter anode aperture (Electrode #2). The result of this work is a detailed paper concerning the arcjet plasma which was published in Journal of Applied Physics.

A larger 1.5 cm diameter anode (Electrode #3) was also tried and found to produce a plasma of twice the diameter of the old. This is about the

limit (for arc-produced plasmas) in size for a fully-ionized plasma which can be obtained with our present pump capacity. This larger plasma (~ 2.5 cm diameter) permits us to observe several instabilities at lower magnetic fields without stabilization by FLR effects. Only a preliminary study of the plasma properties has been made, but Langmuir probe measurements indicate a temperature of ~ 7.5 eV and a density of $\sim 2 \times 10^{14} \text{ cm}^{-3}$ at our present low arc current operation. The resulting β is a $\sim 3\%$ at 2 kG. The larger size should facilitate external excitation of instabilities.

2. Electrostatically Confined, Unmagnetized Plasma

We constructed a large unmagnetized plasma of length ~ 1 m and diameter ~ 40 cm for use in the microwave simulation of laser-plasma interactions as discussed in Section V. This device produces a plasma by a filament-anode discharge as in the standard UCLA DP devices. However, densities comparable to those achieved with surface magnetic confinement are obtained by using the approach of DeGroot²³ in which the chamber walls are biased to repel the primary electrons. Steady-state argon plasmas of density $> 10^{12} \text{ cm}^{-3}$ are obtained in this manner. We have recently constructed an SCR switched capacitor bank which permits the discharge current to be pulsed to quite large values (~ 300 A). We are therefore able to produce critical density plasmas for use with our x-band (10GHz) and S-band (3GHz) microwave sources. This device was used in the heating measurement discussed in Sec. IIIB.3. The present lifetime of 1 msec is limited by the small size of our capacitor bank. We will shortly be adding surface magnetic confinement to this device in the hope of achieving densities $> 5 \times 10^{12} \text{ cm}^{-3}$, on a steady-state or quasi-steady-state basis. This combined confinement scheme has apparently been quite successful in ion thrusters.²⁴ These sources will be employed in the investigation of intense electromagnetic wave interactions with plasmas as described in Section IIIB.

3. Differentially Pumped, Large Diameter, Finite-Beta Magnetized Plasma

Our goals for this system have changed considerably since our last progress report. At that time we were planning on using a 1.2kW, 2.45 GHz cw magnetron to produce the plasma. However, several experiments under consideration, including the study of anomalous resistivity, require a quiescent plasma. Therefore, we are investigating the use of a long duration pulsed hot cathode discharge to produce the desired 7-10 cm diameter, 10^{13} cm^{-3} , 2 m long plasma column. We have chosen LaB_6 as the cathode material as it has large emission and is relatively resistant to "poisoning". The source will be similar to that discussed by Seidl et al²⁵, but will be much larger. The cathode heating will be achieved using the scheme described by Rynn.²⁶ The remainder of the experimental device (vacuum chamber, magnets, etc.) has been assembled and simply awaits the new source.

IV. Publications and Presentations: July 1, 1975 to June 30, 1976

A. Publications (Listing AFOSR Support)

1. "Steady-State, High Density, Magnetized Arc-Jet Plasma Column," J.T. Tang, N.C. Luhmann, Jr., J. Turechek, and D.L. Jassby, Journal of Applied Physics, 46, 3376 (1975)
2. "Destabilization of Hydromagnetic Drift-Alfvén Waves in a Finite Pressure, Collisional Plasma," J.T. Tang and N.C. Luhmann, Jr., Physics of Fluids (to be published).
3. "Measurement of Temperature Fluctuations and Wave Induced Losses Associated with the Drift-Alfvén Instability in a Finite-Beta, Collisional Plasma," J. Holt, N.C. Luhmann, Jr. and J.T. Tang, Journal of Applied Physics (to be published).
4. "Electromagnetic Ion Cyclotron Instability in Current-Carrying Collisional Plasmas," K.F. Lee and N.C. Luhmann, Jr., Plasma Physics (to be published).
5. "Resistive Electrostatic Ion Cyclotron Instability in Plasmas," K.F. Lee and N.C. Luhmann, Jr., IEEE Transactions on Plasma Science PS-4, 40 (1976).
6. "Effects of Finite Bandwidth Driven Pumps on the Parametric Decay Instability," S.P. Obenschain, N.C. Luhmann, Jr. and P.T. Greiling, Phys. Rev. Lett. 36, 1309 (1976).

B. Presentations (Listing AFOSR Support)

1. "Finite-Beta, Current Driven Instabilities," N.C. Luhmann, Jr. Invited Seminar given to U.C. Irvine Physics Dept., 1975.
2. "Electromagnetic Ion Cyclotron Instability in Current-Carrying Collisional Plasmas," K.F. Lee and N.C. Luhmann, Jr., Bull. Am. Phys. Soc. 20, 1379 (1975).
3. "Wave Induced Losses Associated with the Drift-Alfvén Instability in a Collisional Plasma," J. Holt, N.C. Luhmann, Jr. and J. T. Tang, Bull. Am. Phys. Soc. 20, 1307 (1975).
4. "Parametric Instability with a Finite Bandwidth Pump Field: Threshold and Heating," N.C. Luhmann, Jr. and S.P. Obenschain, Bull. Am. Phys. Soc. 20, 1361 (1975).
5. "Experimental Study of Finite-Beta Waves and Instabilities," J. Harslove and N.C. Luhmann, Jr., presented at 1976 IEEE International Conf. on Plasma Science, Austin, Texas.
6. "Effects of Finite Bandwidth on the Interaction of High Power Microwaves with a Critical Density Plasma," N.C. Luhmann, Jr. and S.P. Obenschain, Paper 18, presented at the Sixth Annual Anomalous Absorption Conference, Vancouver, May 1976.

IV. Publications and Presentations: July 1, 1975 to June 30, 1976

B. Presentations (Listing AFOSR Support)

7. "Parametric Instability Threshold and Saturation Level with a Finite Bandwidth Pump," S.P. Obenschain and N.C. Luhmann, Jr., Paper 59, presented at the Sixth Annual Anomalous Absorption Conference, Vancouver, May 1976.

V. Research Personnel

1. N.C. Luhmann, Jr.
2. F.F. Chen
3. Prof. K.F. Lee (Summer Visitor 1975, Chinese Univ. of Hong Kong)
4. Prof. R. Armstrong (Visitor 1976, Tromsø Univ., Norway)
5. J. Hartlove, Graduate Student
6. S. Obenschain, Graduate Student
7. J. Holt, Graduate Student (Graduated Sept. 1975, M.S.)

VI. References

1. R.J.L. Grand, ed., Photon and Particle Interactions with Surfaces in Space, Proceedings, 6th ESLAB Symposium (D. Reidel Pub. Co., Boston, 1973).
2. T.A. Potemra and P.J. Rosenberg, Jour. Geophys. Res. 78, 1572 (1973).
3. G. Müller, W. Friz, and R.S. Palmer, Plasma Phys. 15, 411 (1971).
4. N. Abd el Shahid, P. Deschamps, R. Gravier, and C. Renard, Rev. Sci. Inst. 45, 415 (1974).
5. R.F. Ellis and R.W. Motley, Phys. Fluids 14, 886 (1971).
6. E. Valeo and C. Oberman, Phys. Rev. Lett. 30, 1035 (1973).
7. J.J. Thompson, W.L. Kruer, S.E. Bodner, and J. DeGroot, Phys. Fluids 17, 849 (1974).
8. J.J. Thompson and J.I. Karush, Phys. Fluids 17, 1608 (1974).
9. J.J. Thomson, Nuclear Fusion 15, 237 (1975).
10. G.E. Vekshtein and G.M. Zablavshii, Sov. Phys. Doklady 12, 34 (1967).
11. V.S. Zakharov and G.M. Zablavshii, Sov. Phys. - Tech. Phys. 12, 7 (1967).
12. S. Tamor, Phys. Fluids 16, 1169 (1973).
13. G. Laval, R. Pellar, and D. Pesme, Phys. Rev. Lett. 36, 192 (1976).
14. C. Yamanaka, et al., Phys. Rev. Lett. 32, 1038 (1974).
15. R. Stenzel and A.Y. Wong, Phys. Rev. Lett. 28, 274 (1972).

VI. References

16. S.P. Obenschain, N.C. Luhmann, Jr. and P.T. Greiling, *Phys. Rev. Lett.* 36, 1309 (1976).
17. N.C. Luhmann, Jr. and S.P. Obenschain, Sixth Annual Conf. on Anomalous Absorption, UBS, Paper No. 18 (1976).
18. R.B. Spielman, J.S. DeGroot and D.A. Rasmussen, Univ. of California at Davis Report No. R-8, 1975.
19. D. Arnush, J. Nishikawa, B.D. Fried, C.F. Kennel, and A.Y. Wong, *Phys. Fluids* 16, 2270 (1973).
20. J.J. Thomson, R.J. Faehl, *Phys. Fluids* 17, 973 (1974).
21. J.M. Kindel and C.F. Kennel, *Jour. Geophys. Res.* 76, 3055 (1971).
22. P.K. Chaturvedi and P.K. Kaw, *Plasma Phys.* 17, 447 (1975).
23. R.B. Spielman, J.S. DeGroot, and D.A. Rasmussen, Univ. of Calif. at Davis, Report No. R-8, 1975.
24. A.T. Forrester, private communications.
25. M. Seidl, W. Carr, D. Boyd and R. Jones, *Phys. Fluids* 19, 78 (1976).
26. N. Rynn, *Rev. Sci. Instr.* 40, 1650 (1969).

Report submitted by:

N.C. Luhmann, Jr.
Principal Investigator

Abstract Submitted to the
1976 IEEE International Conference on Plasma Science

May 24-26, 1976

Austin, Texas

Experimental Study of Finite-Beta Waves and Instabilities*

J. Hartlove and N. C. Luhmann, Jr., UCLA

The UCLA arc jet plasma device produces a fully-ionized, steady-state, current-free finite- β plasma column¹. The drift-Alfvén instability was identified in the arc jet plasma and its dispersion properties determined.² The wave-induced losses associated with the instability were also measured³ and compared to both Bohm and classical electron-ion collisional diffusion. More recently, an electromagnetic ion cyclotron instability has been observed which appears to be driven by the field-aligned current in the arc region. Hydromagnetic oscillations at frequencies below the ion cyclotron frequency and its harmonics have been observed with the frequency of the fundamental sometimes being as low as $\Omega_{ci}/2$. Both discrete and continuous mode structure occurs with the discrete structure generally dominating at the lower orders. The lowest order mode has been found to have azimuthal mode number $m=1$ using optical measurements in addition to arrays of electric and magnetic probes. Measurements using shielded magnetic pick-up loops indicate that $\tilde{B}_\theta \gg \tilde{B}_z \gg \tilde{B}_r$. The wave propagates primarily in the azimuthal direction; $k_\theta \gg k_z$, although the exact value of k_θ has not yet been determined accurately.¹¹ The observations are compared with the theoretical predictions for a current-carrying collisional plasma.⁴ In addition, measurements of anomalous resistivity will be presented together with correlations with instability onset.

*Work supported by Air Force Office of Scientific Research Grant 72-2339.

1. J. T. Tang, et al., Jour. of Appl. Physics 46, 3376 (1975)
2. J. T. Tang, et al., Phys. Rev. Lett. 34, 70 (1975)
3. J. Holt, et al., Bull. Am. Phys. Soc. 20, 1307 (1975)
4. K. F. Lee and N. C. Luhmann, Jr., Bull. Am. Phys. Soc. 20, 1379 (1975)

Parametric Instability Threshold and Saturation Level with a Finite Bandwidth Pump.*
S.P. OBENSCHAIN AND N.C. LUHMANN, JR., Univ. of California, Los Angeles.--Experimental results will be presented where several different randomly and coherently modulated pumps are employed to drive the parametric decay instability. In the wide bandwidth limit, where the pump bandwidth $\Delta\omega$ is much larger than the instability resonance width γ , we find agreement with theory in that the threshold power, growth rate and saturation level of the instability are determined by that fraction of the spectral distribution of the pump contained within the instability resonance width.¹ Thus we obtain significantly increased thresholds and reduced saturation levels for the instability when wide bandwidth pumps are employed. For narrower bandwidths, $\Delta\omega < \gamma$, coherent phase modulation of the pump appears to change the instability mechanism.

*Work supported by Air Force Office of Scientific Research Grant 72-2339

¹J.J. Thomson, Nucl. Fusion 15, 237 (1975).

University of California
Electrical Sciences and Engineering Department
7731 Boelter Hall
Los Angeles, CA 90024

Effects of Finite Bandwidth on the Interaction of High Power Microwaves with a Critical Density Plasma.*
N. C. LUHMANN, JR. AND S. P. OBENSCHAIN, Univ. of California, Los Angeles.--Results are presented concerning the effects of a finite bandwidth pump on the interaction of high power microwaves with a near critical density plasma. We include a study of the heating due to the excitation of parametric instabilities when the pump power greatly exceeds the threshold power level. At these high power levels, modification of the plasma spatial profile due to radiation pressure is significant. Finite bandwidth can modify this as there is then not a distinct critical layer ($\omega \approx \omega_{pe}$) where the radiation pressure forces are concentrated.

*Work supported by Air Force Office of Scientific Research Grant 72-2339

University of California
Electrical Sciences and Engineering Dept.
7731 Boelter Hall
Los Angeles, CA 90024

sity of completely stripped oxygen ions are not known.

In conclusion, radial profiles of low-ionization-degree impurity ions and of highly ionized ions have been obtained. We have shown that these profiles can be used in order to deduce impurity fluxes and that the values obtained for the oxygen ions in the outer plasma shell agree reasonably well with the theoretical ones. It must be pointed out, however, that, from particle- and energy-balance considerations, it has been previously shown that these large fluxes cannot reach the plasma center.³

*C. Breton, J. Breton, Ph. Brossier, J. P. Bussac, R. Cano, M. Chateller, M. Cotsaftis, J. P. Creun, R. Del Cas, C. De Michelis, P. Ginot, J. P. Girard, R. Gravier, F. Hennion, F. Koechlin, D. Launois, P. Lecoustey, J. Lelegard, E. Maschke, M. Mattioli, C. Mercler, P. Morlette, R. Papoular, P. Platz, P. Plinate, C. Renaud, A. Samain, A. Schram, Z. Sledziew-

ski, P. Smeulders, J. L. Soule, J. Tachon, A. Torosian, J. Touche, D. Veron, F. Werkoff, and B. Zaufagna.

¹E. Hinnoy, L. C. Johnson, E. B. Meservey, and D. L. Dimock, *Plasma Phys.* **14**, 755 (1972).

²N. Bretz, D. L. Dimock, E. Hinnoy, and E. B. Meservey, *Nucl. Fusion* **15**, 313 (1975).

³Equipe TFR, *Nucl. Fusion* **15**, 1053 (1975).

⁴V. I. Gervids and V. A. Krupin, *Pis'ma Zh. Eksp. Teor. Fiz.* **18**, 106 (1973) [*JETP Lett.* **18**, 60 (1973)].

⁵S. A. Cohen, J. L. Cecchi, and E. S. Marmor, *Phys. Rev. Lett.* **35**, 1507 (1975).

⁶E. Hinnoy and F. W. Hofmann, *J. Opt. Soc. Am.* **53**, 1259 (1963).

⁷More accurate measurements are necessary in order to know if this density increase is due to excitation of recombining ions.

⁸M. Mattioli, EURATOM-CEA Association, Fontenay-aux-Roses, Report No. E.U.R.-C.E.A.-F.C. 761, 1975 (unpublished).

⁹P. H. Rutherford, *Phys. Fluids* **17**, 1782 (1974).

¹⁰TFR Group, in *Proceedings of the Fifth International Conference on Plasma Physics and Controlled Nuclear Fusion Research, Tokyo, 1974* (International Atomic Energy Agency, Vienna, 1975), Vol. I, p. 135.

Effects of Finite-Bandwidth Driver Pumps on the Parametric-Decay Instability*

S. P. Obenschain, N. C. Luhmann, Jr., and P. T. Greiling

University of California, Los Angeles, California 90024

(Received 17 February 1976)

The effects of a finite-bandwidth driver pump on the parametric-decay instability are investigated experimentally. The results include the dependence of threshold power, growth rate, and saturation level on the bandwidth of several coherently and randomly modulated pumps.

Parametric instabilities of both the absorptive and reflective types may have serious consequences for laser-pellet fusion and laser or rf heating of magnetically confined plasmas. There has therefore been considerable interest in means to increase the instability thresholds and reduce the growth rates. A proposed solution is to properly shape the bandwidth characteristics of the pump.¹⁻³ Theoretical investigations^{4,5} indicate that for the case of a randomly modulated pump whose energy is uniformly distributed over a bandwidth $\Delta\omega$ much larger than the instability resonance width γ , the effective power available to excite the instability is related to the incident power P_0 by $P_{\text{eff}} = \gamma/\Delta\omega P_0$. In this large-bandwidth limit ($\Delta\omega \gg \gamma$), the precise mechanism responsible for producing the finite-bandwidth pump has been found to be rather unimportant in terms

of the effects on threshold and growth rate.¹ In the present discussion the effective power is defined to be that fraction of the spectral energy distribution of the pump contained within the instability resonance width. This definition provides a means to compare pumps with various continuous as well as discrete spectral distributions. A simple extension of present theory therefore suggests that the effective power as defined above should determine the threshold, growth rate, and saturation level regardless of the bandwidth mechanism. It should be noted, however, that the resonance width increases with increasing pump power and plasma inhomogeneity, so that for laser-pellet interactions the realizable widths may be more nearly comparable ($\Delta\omega \approx \gamma$). In this case, one expects the particular bandwidth mechanism to be important. For the

experiment described herein, we employed several distinctively different finite-bandwidth mechanisms to explore the effect on the decay instability.

The experiments were performed in an unmagnetized, electrostatically confined, filament-discharge plasma⁶ of 100 cm length and 35 cm diam with argon fill pressures of 0.4 mTorr. Typical plasma parameters are electron temperature $kT_e \sim 2-3$ eV, temperature ratio $T_e/T_i \sim 8-10$, plasma density $n_e = (2-18) \times 10^9$ cm⁻³, and total background fluctuation level $\Delta n/n < 0.1\%$. The rf driver pump (frequency $\omega_0 > \omega_{pe}$) is introduced by means of a gridded parallel-plate capacitor system (5 cm diam grids with 3 cm spacing) similar to that of Stenzel and Wong.⁷ Plasma density and temperature are monitored using both Langmuir probes and a retarding-grid electrostatic energy analyzer. Movable shielded double probes are used to detect the excited ion waves; the high-frequency decay waves are monitored by coaxial probes shielded from direct rf pickup. Upon application of rf power to the grids, a well-defined ion disturbance ($\Omega_i/2\pi \approx 400$ kHz) appears when the power exceeds a distinct threshold value. The ion fluctuations are accompanied by high-frequency sideband decay waves ω_s . The observed value of the threshold power together with frequency matching ($\omega_0 = \omega_s + \Omega_i$) and phase-velocity measurements indicate that the parametric decay instability is excited by the pump.

The resonance width of the instability, as determined by a narrow-band pump, is typically $\sim 1\%$ of the pump center frequency. Here the resonance width is defined as the full width of the threshold power curve at the twice-power points. This observed width is much larger than that calculated from uniform plasma theory ($\leq 0.1\%$) and is due, we believe, to the gentle density gradients ($\sim 2\%/cm$ over several centimeters) produced by the insertion of the grids into our otherwise uniform plasma and to the finite-size interaction region.

Several different finite-bandwidth pumps are employed in this experiment. By mixing narrow-band rf with white Gaussian noise in a balanced mixer, rf of adjustable bandwidth is produced, where the bandwidth arises from both amplitude and phase modulation. Another source produces a pump whose bandwidth is primarily due to phase modulation. The rf field of this source is given by $E(t) = \cos[\omega_0 t + \alpha(t)]$, where $\alpha(t)$ is the particular phase modulation function. The pure phase-modulation results reported herein are concerned

with either the case of coherent sinusoidal phase modulation, with $\alpha(t) = x \cos(\omega_m t)$, where ω_m is the modulation frequency and x the modulation index, or the case of random-noise phase modulation. The noise modulation employed is Gaussian white noise of adjustable amplitude and bandwidth.

For the case of sinusoidal phase modulation, the rf field may be expanded in terms of Bessel functions. Its Fourier spectrum then consists of the fundamental with amplitude proportional to $J_0(x)$ and modulation sidebands of amplitude $J_n(x)$ and frequency $\omega = \omega_0 \pm n\omega_m$, where n is an integer. When $\omega_m \gg \gamma$ and ω_0 has been adjusted to coincide with the frequency for minimum threshold, the effective power P_{eff} is just $J_0^2(x)P_0$. Theory⁸ therefore predicts the threshold power to be a function of the modulation index:

$$P_{\text{thres}}(x) = J_0^{-2}(x)P_{\text{thres}}(0).$$

In Fig. 1(a), the experimentally determined threshold power normalized to the narrow-band threshold is plotted as a function of the modula-

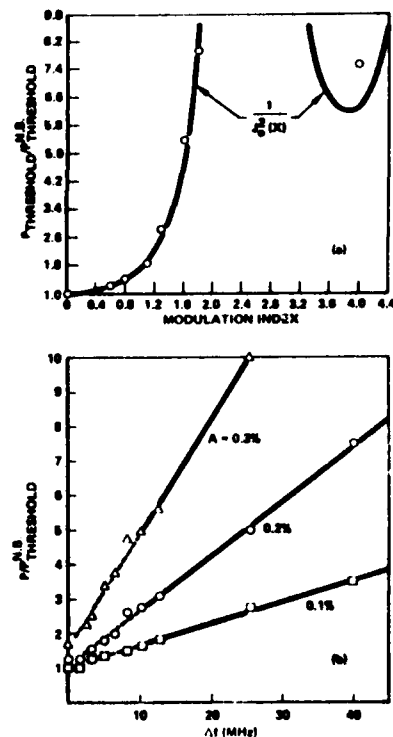


FIG. 1. (a) Threshold power normalized to the narrow-band threshold as a function of modulation index for a sinusoidally phase-modulation pump ($\omega_m > \gamma$). (b) Pump power (normalized to the narrow-band threshold) required to produce a given density-fluctuation level A as a function of the width of the balanced-mixer-produced noise pump.

tion index for the case $\omega_m \gg \gamma$. Note the agreement between theory and experiment, even at large modulation index, including a point within the second cycle of the Bessel function.

Figure 1(b) illustrates similar results for the balanced-mixer-produced noise pump. In this case, the power necessary to achieve a given normalized density-fluctuation amplitude A is plotted as a function of the pump bandwidth $\Delta f = \Delta\omega/2\pi$. Here A is defined by $A = (n_i T)^{-1} \int_0^T |\Delta n_i| \times dt$, where T is large compared to the wave growth times and Δn_i is the total density-fluctuation level in the frequency range of the parametric-decay-instability produced ion waves [~ 0.1 – 1 MHz]. The lowest amplitude, $A = 0.1\%$, corresponds to the threshold level where the instability first appears distinctively above the background fluctuations. In the limit $\Delta\omega \gg \gamma$, theory^{1,4} predicts that for the threshold power and pump bandwidth $\Delta\omega$ are linearly related. Over the range of power levels and bandwidths investigated, this relation was found to be approximately satisfied not only for the instability threshold power, but also for the power necessary to achieve a given level of saturated density fluctuations. The straight line fit to the data presented in Fig. 1(b) is evidence of the validity of the theory. The nonzero intercept of the lines for $\Delta\omega = 0$ is indicative of the limitations of the theory which does not take account of the precise interaction of the pump at frequencies outside the resonance region. An estimate of the instability resonance width at each fluctuation level may be obtained from the slope of the lines in Fig. 1(b). Alternatively, the resonance width may be obtained directly by varying the frequency of the narrow-band pump and observing the width of the instability curve at the twice-power points for a given fluctuation level. The results obtained from both techniques are compared in Table I and are found to be in reasonable agreement. Similar re-

TABLE I. Instability resonance width $\Delta\omega/2\pi$.

Fluctuation level (%)	Resonance width ^a (MHz)	Resonance width ^b (MHz)
0.1	25	16
0.2	14	8
0.3	8	6

^aResonance width determined using narrow-band pump.

^bResonance width obtained from slopes in Fig. 1(b).

sults were obtained for the purely phase-modulated noise pump.

Detailed studies of the saturated level of the instability as a function of pump center frequency, power, and bandwidth were also made. In Figs. 2 and 3, experimental scans of the normalized density-fluctuation level A are displayed as a function of pump frequency and power for both noise and sinusoidally phase modulated pumps. The width $\Delta\omega/\omega_0$ of the noise phase-modulated pump is varied from $\sim 0\%$ to 1.2% in Fig. 2, while the pump power is increased from 0.5 to 2 W in 0.5 W increments. Increased thresholds and decreased saturated levels are evident as the bandwidth is increased beyond the instability resonance width. Results of measurements of saturated density-fluctuation levels obtained by successively increasing the modulation index of the sinusoidally phase-modulated pump ($\omega_m > \gamma$) are shown in Fig. 3. In this case only the results from two pump power levels are displayed. These latter results clearly illustrate that while coherent pump modulation can increase the threshold

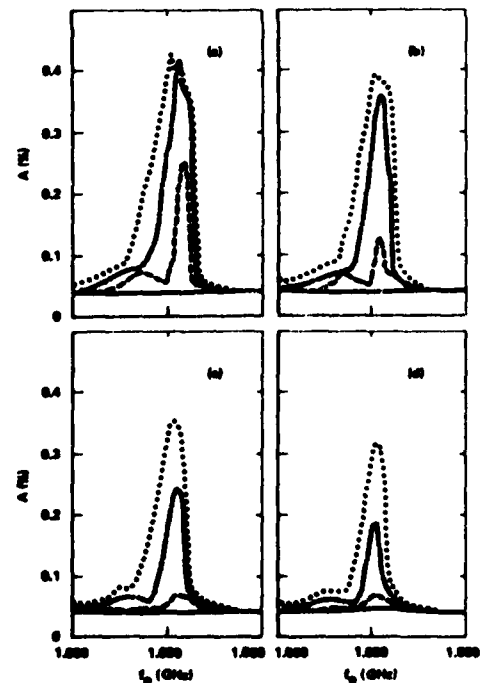


FIG. 2. Saturated density fluctuation level A as a function of pump power and center frequency for the noise phase-modulated pump. The noise bandwidth $\Delta\omega/2\pi$ is < 10 kHz for (a), 3 MHz for (b), 6 MHz for (c), and 12 MHz for (d). Pump power is varied from 0.5 to 2.0 W: —, 0.5 W; ---, 1.0 W; - - -, 1.5 W; and ···, 2.0 W.

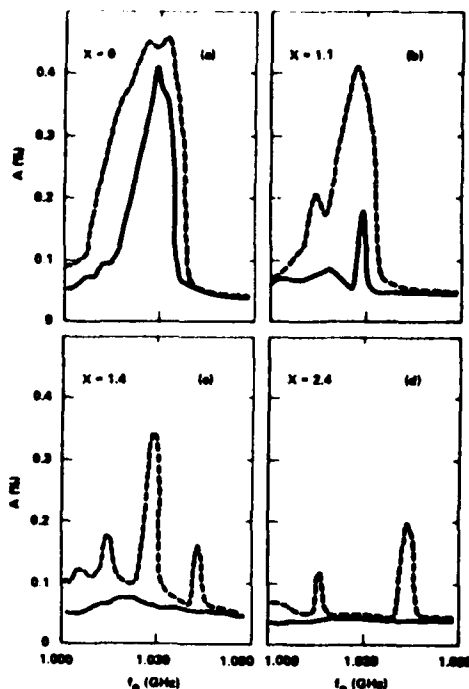


FIG. 3. Saturated density-fluctuation level A as a function of pump power and center frequency for the sinusoidally phase-modulated pump ($\omega_m/2\pi = 14$ MHz $>$ $\gamma/2\pi$). The modulation index is $x = 0$ for (a), $x = 1.1$ for (b), $x = 1.4$ for (c), and $x = 2.4$ for (d). For $x = 1.4$ the pump power is distributed approximately equally between the center frequency and the first upper and lower modulation sidebands, while for $x = 2.4$ the power at the center frequency is approximately zero. Two values of pump power are shown: —, 2.0 W, and ---, 4.0 W.

and decrease the saturation level for pumps tuned to threshold minimum, it can have the opposite effect at multiples of the modulation frequency.

The instability growth rate dependence upon bandwidth was also investigated. The results were consistent with predictions in that the insta-

bility behaves as if only the power contained within the resonance width were applied.

When the pump bandwidth $\Delta\omega$ becomes comparable to γ , we find little change in the instability threshold, growth rate, and saturation level from the narrow-band case. However, there does appear to be a change in the instability mechanism. For the case of sinusoidal phase modulation with $\omega_m \lesssim \gamma$, each of the main spectral components of the pump can have decay sidebands, indicating a higher-order bootstrapping process. These additional sidebands are not observed for $\omega_m \gg \gamma$. Details of the region $\Delta\omega \lesssim \gamma$ will be presented elsewhere.

In conclusion, our results for wide-bandwidth pumps ($\Delta\omega \gg \gamma$) are consistent with theoretical predictions. Interesting effects occur for narrower bandwidths, and further theoretical and experimental investigations appear justified.

It is a pleasure to acknowledge useful discussions with Dr. R. Stenzel, Professor J. S. DeGroot, Dr. J. J. Thomson, and Professor F. F. Chen. The participation of Mr. M. Herbst and Mr. D. Yang in the early stages of the experiment together with the expert technical assistance of Mr. D. Cook is appreciated.

*Work supported in part by U. S. Air Force Office of Scientific Research under Grant No. 72-2339.

¹J. J. Thomson, Nucl. Fusion **15**, 237 (1975).

²E. J. Valeo and C. R. Oberman, Phys. Rev. Lett. **30**, 1035 (1973).

³J. J. Thomson, W. L. Kruer, S. E. Bodner, and J. S. DeGroot, Phys. Fluids **17**, 849 (1971).

⁴J. J. Thomson and J. I. Karush, Phys. Fluids **17**, 1608 (1974).

⁵G. Laval, R. Pellat, and D. Pesme, Phys. Rev. Lett. **36**, 192 (1976).

⁶R. B. Spielman, J. S. DeGroot, and D. A. Rasmussen, University of California at Davis Report No. R-8, 1975 (unpublished).

⁷R. Stenzel and A. Y. Wong, Phys. Rev. Lett. **28**, 274 (1972).